

Janne Esa

**Fuel and economic efficiency of an
ice-going vessel on the Northern Sea
Route**

School of Engineering

Thesis submitted for examination for the degree of Master of Science in Technology.

Espoo 25.5.2015

Thesis supervisor:

Professor Pentti Kujala

Thesis advisor:

Lauri Kuuliala, M.Sc. (Tech.)

Author: Janne Esa		
Title: Fuel and economic efficiency of an ice-going vessel on the Northern Sea Route		
Date: 25.5.2015	Language: English	Number of pages: 9+90
Department of Applied Mechanics		
Major: Marine Technology		Code: K3005
Supervisor: Professor Pentti Kujala		
Advisor: Lauri Kuuliala, M.Sc. (Tech.)		
<p>In this thesis fuel and economic efficiency of an ice-going vessel were studied. The study was carried out for a double acting ship (DAS) and an ice-bow vessel operating year-around on the Northern Sea Route (NSR). For comparison these efficiencies were investigated for an open water vessel operating on the Suez Canal route (SCR) and a vessel using the NSR during operable months, <i>i.e.</i>, from July until December and rest of the year using the SCR. These are the months permitted by current NSR regulations.</p> <p>The fuel consumption of the vessel was studied with the transit-simulation. For DAS and the ice-bow ship first the speed was solved in different ice conditions. For open water and assisted ships the power demand was calculated. DAS and ice-bow ship were assumed to use full power in ice and the speeds in open water and ice channel were assumed to be constant. The fuel consumption was limited to the consumption caused by the ship movement, <i>i.e.</i>, no consumption caused by lighting, heating <i>etc.</i> were taken into account. For resistance calculations the resistance equations for open water, level ice, ice ridges and channel ice were used. For economical calculations only voyage and some operational costs were taken into account. For simulating the performance of the DAS, the ice field was generated with two different methods: the one presented by La Prairie and the one by Kotovirta. This is done in order to compare these two methods.</p> <p>The results indicate that the NSR is a potential route for shipping during an average winter with DAS but not with an ice-bow ship. DAS is the most fuel efficient option on average winter. During severe winter, using the SCR year-around is the best option. The ice ridge generating methods presented by La Prairie and Kotovirta gives quite similar speeds. However, method of Kotovirta gives more optimistic results what comes to the cases the ship got stuck in ice. Due to the limited number of studies of the performance of a double acting ship, <i>e.g.</i>, the lack of studies about the performance of a DAS in ice ridges, the results should be validated with model tests.</p>		
Keywords: Ice-going vessel, fuel efficiency, economical efficiency, ridge generator, equivalent ridge thickness, Northern Sea Route, Suez Canal route, ice resistance, transit-simulation		

Tekijä: Janne Esa				
Työn nimi: Jäissä kulkevan laivan polttoaine- ja taloustehokkuus Koillisväylällä				
Päivämäärä: 25.5.2015	Kieli: Englanti	Sivumäärä: 9+90		
Sovelletun mekaniikan laitos				
Pääaine: Meriteknikka	Koodi: K3005			
Valvoja: Professori Pentti Kujala				
Ohjaaja: DI Lauri Kuuliala				
<p>Tässä työssä tarkastellaan jäissä kulkevan laivan polttoaine- ja taloustehokkuutta Koillisväylällä. Tarkasteluun otettiin ympäri vuoden Koillisväylää käyttävä, jäissä peruuttaen ja avovedessä keula edellä operoiva laiva, niin sanottu DAS -konsepti, sekä keula edellä operoiva jääkeulalla varustettu laiva. Tehokkuusvertailu suoritettiin myös ympäri vuoden Suezin kanavaa käyttävälle avovesilaivalle sekä nyksäännöt täytävälle alukselle, joka käyttää Koillisväylää lain sallimat kuukaudet jäänmurtajan avustamana ja Suezin kanavaa loppuajan.</p> <p>Polttoaineenkulutus selvitettiin suorituskyksimuloinnin avulla. DASin ja jääkeulalaivan nopeus eri jääolosuhteissa ratkaistiin ja muille laivoille selvitettiin tehovaatimus. DASin ja jääkeulalaivan oletettiin operoivan täydellä teholla jäissä. Avovedessä ja rännissä nopeuden oletettiin olevan vakio. Kulutus rajattiin käsittämään ainoastaan laivan ajosta aiheutuva, ts. tarkastelun ulkopuolelle jätettiin lämmitys, sähkölaitteet jne. Simuloinneissa käytettiin vastuskaavoja avovedessä, tasaisessa jäissä, jäävallissa sekä -rännissä. Taloustehokkuus rajattiin käsittämään liikennöinti- sekä operointikustannukset. DASin simuloinnissa jääröntä luotiin kahdella eri menetelmällä, La Prairie ja Kotovirta. Tämä tehtiin menetelmien yhdenmukaisuuden vertaamiseksi.</p> <p>Tulokset osoittavat Koillisväylän ympäri vuotisen käytön olevan perusteltua keskimääräisenä jäätalvena DAS:illa, jolloin tämä osoittautui polttoainetehokkaimaksi, mutta ei jääkeulalaivalla. Ankarana talvena Suezin kanavan kautta liikennöinti ympäri vuoden osoittautui parhaaksi vaihtoehdoksi niin polttoaine- kuin taloustehokkuuden kannalta. Molemmat jäävallien luontimenetelmät antoivat varsin samanlaisia tuloksia laivan nopeudesta jäissä. Kotovirta antoi kuitenkin optimistisempia tuloksia, mitä tulee kertoihin, jolloin laiva juuttui jääröntään. DAS:in simuloointia on kuvattu hyvin vähän julkaisuissa, ja esimerkiksi suorituskykyä vallikentässä ei ole tarkasteltu lainkaan. Tässä työssä käytetyt menetelmät tulisi validoida mallikokein, jotta niiden paikkansapitävyys voittaisiin osoittaa.</p> <p>Avainsanat: Jäissä kulkeva laiva, polttoaine- ja taloustehokkuus, vallikentän luonti, ekvivalentti jäärönsuus, Koillisväylä, Suezin kanava, jäävastus, suorituskyksimulointi</p>				

Preface

I would like to thank professor Pentti Kujala for giving me the possibility to work with this interesting topic and also supervising this thesis. This thesis was funded through the JOULES-project, and I would like to thank the cooperative people and companies involved in the project, especially Tommi Heikkilä from Aker Arctic and Kari Sillanpää from Meyer Turku deserve to be mentioned.

I would also like to express my very great appreciation to Lauri Kuuliala for his invaluable support as my thesis advisor. Especially his help with the simulation process and comments during the work had significant effect on the outcome of this thesis.

I owe great gratitude to Ville Viitanen for proofreading this thesis and for the significant help with the matlab routines, in addition to being a good friend through our studies.

I also express my gratefulness to my brother, Jaakko, to being a perfect brother and for the awesome sparring sessions where I was literally able to kick and hit the thesis related stress out of me.

My parents, Hannu and Sirpa, deserve my great appreciation for helping me economically and guiding me through my studies, in addition for all the support and encouragement with all in my life. I am also thankful to all my friends and family, not forgetting Frodo and the Tontunmäen mafia.

Espoo, 25.5.2015

Janne E. Esa

Contents

Abstract	ii
Abstract (in Finnish)	iii
Preface	iv
Contents	v
Symbols and abbreviations	vii
1 Introduction	1
2 Rules and regulations as a motivation to reduce fuel consumption	5
2.1 EEDI and SEEMP	6
2.2 Ways to improve fuel efficiency	7
3 State of the art for Northern Sea Route and transit-simulation studies	9
3.1 Northern Sea Route -studies	9
3.2 Transit-simulation	11
3.3 Summary	12
4 Sea ice on the Northern Sea Route	14
4.1 Ice conditions used in the thesis	14
4.2 Level ice	16
4.3 Ice channel	17
4.4 Ice ridge	18
5 Ice-going vessel characteristics	20
5.1 Icebreaking	20
5.2 Designing basics	22
5.3 Double acting ship	24
6 Modelled ship concepts	25
7 Investigated routes	28
7.1 Route planning	29
7.2 Northern Sea Route	30
7.3 Suez Canal route	34
8 Modelling methods	35
8.1 Generating the ice field	35
8.2 Transit-simulation	39
8.2.1 Resistance equations	41
8.2.2 Channel resistance	45

8.2.3	Open water resistance	47
8.3	Models to solve fuel and economic efficiency	48
8.3.1	Fuel consumption	48
8.3.2	Economical model	52
9	Results	55
9.1	DAS	55
9.2	Ice-bow ship	61
9.3	Open water ship	62
9.4	Assisted ship	63
9.5	Comparing results	64
10	Analyses of the results	68
10.1	La Prairie vs Kotovirta	68
10.2	Fuel efficiency	70
10.3	Economical efficiency	71
10.4	Summary	72
11	Conclusions	73
	Bibliography	76
A	Ice data	81

Symbols and abbreviations

Symbols

\mathbf{a}	Acceleration vector
A_{WF}	Waterline area of the foreship
B	Breadth of the ship
CD	Canal due
C_m	Midship section coefficient
C	Concentration
C_p	Prismatic coefficient
C_{R_{sA}/R_s}	Astern-mode coefficient in ice ridge
C_{USD}	Cost
C_w	Waterplane area coefficient
FC	Fuel cost
Fn	Froude number
g	Gravitational constant
h_{eq}	Equivalent ridge thickness
H_F	Thickness of the displaced brash ice
H_{ice}	Level ice thickness
H_{keel}	Keel depth
H_M	Thickness of the brash ice
H_r	Ridge depth
IC	Icebreaking cost
K_0	Coefficient of lateral stress at rest
K_P	Coefficient of passive stress
\dot{m}_{fuel}	Fuel consumption
L	Length of the ship
L_{wl}	Length of the waterline
L_{bow}	Length of the bow
L_{stern}	Length of the stern
L_{par}	Length of the parallel midship
OC	Operational cost
$P_{propulsion}$	Propulsion power
R_A	Model-ship correlation resistance
R_{APP}	Resistance of appendages
R_b	Bending resistance
R_B	Additional pressure resistance of bulbous bow near the water surface
R_{bow}	Bow resistance in ice ridge
R_c	Crushing resistance
R_{ch}	Channel resistance
R_F	Frictional resistance
$R_{ice}^{Lindqvist}$	Level ice resistance
R_{par}	Parallel midbody resistance in ice ridge
R_{ridge}	Ridge resistance
R_s	Submergence resistance
R_{sA}	Submergence resistance in astern-mode
R_{total}	Open water resistance
R_{TR}	Additional pressure resistance immersed transom stern
R_W	Wave-making and wave-breaking resistance

s_0	Initial position vector
s	Final position vector
T	Draft of the ship
T_{net}	Net thrust
v_0	Initial velocity vector
v	Final velocity vector
v_{ow}	Open water speed
x	Distance between two ridges
α	Waterline angle
δ	Slope angle of the side wall of the brash ice
Δt	Time interval
κ	Keel angle
μ_H	Coefficient of friction between the ice and the hull
μ_s	Ridge density
ν	Poisson's ratio
ρ_{ice}	Ice density
ρ_{water}	Water density
σ_b	Ice bending strength
ϕ	Stem angle
Φ	Internal friction angle

Abbreviations

CO ₂	Carbon Dioxide
CSMF	Comparative Ship Merit Factor
DAS	Double Acting Ship
ECA	Emission Control Area
EEDI	Energy Efficient Design Index
GHG	Greenhouse Gas
HFO	Heavy Fuel Oil
IMO	International Maritime Organization
IRIS	Ice Ridging Information System
JOULES	Joint Operation for Ultra Low Emission Shipping
LNG	Liquid Natural Gas
MDO	Marine Diesel Oil
MOH	Marine Operations Headquarters
NO _x	Nitrogen Oxide
NSR	Northern Sea Route
PM	Particulate Matter
RFR	Required Freight Rate
S	Sulfur
SCR	Suez Canal Route
SD	Standard Deviation
SECA	Sulfur oxide Emission Control Area
SEEMP	Ship Energy Efficiency Management Plan
SMF	Ship Merit Factor
SO _x	Sulfur Oxide
TEU	Twenty-foot Equivalent Unit
UN	United Nations
USD	US Dollar
WHR	Waste Heat Recovery
WMO	World Meteorology Organization

Chapter 1

Introduction

In the late 20th century the world woke to consequences of global warming (NASA 2015). That led to growing interest to reduce greenhouse gases (GHG) and other emissions caused by industry. This drove to find ways to reduce emissions and to stop global warming, which culminated in new rules and regulations. However, one consequence of global warming was melting of the sea ice. Melting ice has made the Arctic Sea a notable alternative for shipping industry because it brings Europe and Asia closer together. It shortens the shipping route almost 8000 km compared to route via the Suez Canal (Way et al. 2015). Decreased amount of ice has made the Arctic Sea also notable area for gas and oil companies for business.

Reducing fuel consumption of shipping is the goal that both the shipping company and the regulation officer, aim at. Most of the emissions, such as CO₂, essentially depend on fuel consumption (van Basshuysen and Schäfer 2004). Price of the fuel is a significant part of the operational costs for shipowner and therefore operations should be planned to be as fuel efficient as possible. In this thesis fuel efficiency for different routes and concepts is studied. After that also the economic efficiency is examined to compare the fuel efficiency to the economic one. The studied cases are:

- A double acting ship (DAS) -concept that operates independently year-around on the Northern Sea Route (NSR). If it gets stuck in ice on some area, it is escorted through it by an icebreaker. This vessel is called DAS.
- A vessel with an ice-bow operating independently year-around on the NSR. This vessel is called ice-bow ship.
- An open water ship that operates year-around via the Suez Canal route (SCR). Later on this vessel is called open water ship.
- A vessel with an ice-bow, which operates along the NSR on months permitted by law, *i.e.*, from July until late November (Northern Sea Route Information Office 2015).

Rest of the year the vessel operates along the SCR. Assumption is that the vessel is escorted by an icebreaker through ice. Later called assisted ship.

Above mentioned cases have been chosen to compare the effectiveness of the DAS-concept in ice to a typical ice-bow vessel. Open water ship using the SCR is taken into account to compare two different routes connecting Europe to Asia. Due to the rules of the navigation on the NSR, currently a vessel could not be sailing independently year-around there and therefore an assisted ship is also taken into account to the study. All the case vessels have the same power and the chosen ice class is Arc4 (1A). In this thesis, the ice class affects only to the used rules for the vessel on the NSR. With ice class Arc4, a ship can operate on the NSR from July until late November assisted by an icebreaker. Therefore, year-around operations would not be possible, but in this thesis this is investigated to see the potential of a double acting ship to use the NSR year-around.

DAS and open water ship are similar vessels; with the same parameters, both have a bulbous-bow *etc*. The idea of a double acting concept is that it moves stern-first in ice and therefore can have an open-water bow. Double acting -concept is explained in Chapter 5. Ice-bow and assisted ship are similar to DAS and open water ship except they do not have a bulb and therefore the open water resistance is expected to be higher (Matusiak 2010). These concepts are presented closer in Chapter 6. Fuel and economical efficiency are solved for each case.

Fuel consumption is solved on the NSR for two different winters, *i.e.*, two different ice conditions. These conditions are explained in Chapter 4. The consumption is calculated based on power demand on each case. In ice the power demand is assumed to be the full propulsion power of the vessel and therefore the vessel speed in different conditions on the route is solved. After the vessel speed is known, time spent on route can be calculated, and hence the fuel consumption can be evaluated. For open water ship the speed is assumed to be constant, 8.5 m/s. For economic calculations consumed fuel price, route fees, icebreaker support and operational costs are taken into account. The target is to find the voyage cost to ship one TEU from Europe to Asia. Fuel consumption is limited to the one caused by the ship movement, *i.e.*, amount of fuel consumed to overcome the resistance and no consumption due to, *e.g.*, heating, lightning *etc.* is taken into account.

Assumption is that the DA-concept operates stern-first in ice with full power. Operation is mainly independent. Also performance for 80 % of power on average winter is investigated to see how the power reduction, *i.e.*, slow-steaming, affects to the performance and fuel efficiency of this vessel. Ice field built for the performance simulations contains both level ice and ice ridges. The ice field is generated with the method presented by La Prairie et al. (1995). With this method the ice field can be modelled quite realistically and the

field contains a random number of ridges which corresponds to the input ridge density after multiple simulations. Input data for the method is mean ridge thickness, ridge density, keel angle and the maximum ridge thickness. Consolidated layer of ridges is assumed to be 1.5 times the thickness of the surrounding level ice (Kujala and Riska 2010). For comparison the ice field is also built with the method presented by Kotovirta et al. (2009). This method flattens ridges to cover the whole ice field, *i.e.*, whole field consists of level ice and ridges with solved equivalent thickness and therefore is faster for simulations. This method uses mean ridge thickness, ridge density and keel angle as input data, *i.e.*, it does not take the maximum ridge thickness into account. These methods are described closer in Chapter 8.

In Chapter 2, rules and regulations to decrease emissions of the shipping industry are presented briefly. In Chapter 3, the state of the art is divided between the ones related to studies done of NSR operations and for the ones where transit-simulation is used and studied. In Chapter 4, sea ice is presented; shortly the formation and different conditions. Condition description is limited to the ones needed for the simulations done in this thesis. In Chapter 5, an ice-going vessel is described. Also the double-acting concept is clarified. In Chapter 6, used vessel dimensions are presented. Chapter 7 concentrates to describe the used routes; SCR and NSR. The characteristics and limitations of both routes are described. In Chapter 8, equations for the simulations are presented. Also the simulation model and the generation methods for the ridge field are presented in the chapter. In Chapter 9, the simulation results are presented. Chapter 10 is for analysis and Chapter 11 for conclusions of the subject.

This thesis is funded by a project called Joint Operation for Ultra Low Emission Shipping (JOULES). JOULES is a European Union (EU) project. Aim of the project is accepting future challenges for European Maritime Industry to significantly reduce energy consumption, emission of climate gases and other harmful emissions to air (JOULES 2015). Task of JOULES is to modify a baseline vessel to reduce CO₂ by year 2025 and 2050. The baseline vessel used in this thesis is an assisted ship operating between Rotterdam and Busan via the Northern Sea Route.

Aim of the thesis

- To have an understanding of the difference of the routes connecting Europe to Asia.
- To investigate the performance of a double acting ship in ice. The performance of a double acting -concept has only slightly been simulated in previous publications. There are no publications where the performance of a DAS have been compared on the NSR and on the SCR. Neither the performance of the DAS in a ridge field has been studied before in publications.

- To get some idea of different ways for shipping between Europe and Asia and find the most feasible one, taking into account both fuel and economic efficiency.
- To compare results with ridge fields built for transit-simulation with two methods, the ones presented by La Prairie and Kotovirta. These methods have not been compared before.

Chapter 2

Rules and regulations as a motivation to reduce fuel consumption

In this chapter, different rules and regulations that drive shipowners to find more fuel and energy efficient ways for operations are described briefly. At the end of this chapter, ways to reduce fuel consumption are described.

There are multiple agencies and organizations, both local and global, to maintain and develop rules and regulations to make marine traffic and operations cleaner and safer. The International Maritime Organization (IMO) is a specialized agency of the United Nations (UN) whose role is to create a level-playing-field, so that ship operators cannot address their financial issues by simply cutting corners and compromising on safety, security and environmental performance. The IMO measures cover ship design, construction equipment, manning, operation and disposal to ensure that shipping remains safe, environmentally sound, energy efficient and secure. (IMO 2015)

Shipping causes 2.7 % of world's CO₂ emissions (Hasan 2011). IMO and national environmental agencies have set a goal to drastically reduce engine exhaust emissions and green house gases (GHG). These new rules are impacting ships that engage in international and coastal shipping trade, cruise industry and shipowners and operators.

There are sea areas where ships have to fulfill specific regulations to get permission to operate and do business. These areas are called Emission Control Area (ECA) and Sulfur Oxide (SO_x) Emission Control Area (SECA). The rules for these areas will mandate reductions in emissions of sulfur (S), nitrogen oxide (NO_x) and particulate matter (PM). (McGill et al. 2013)

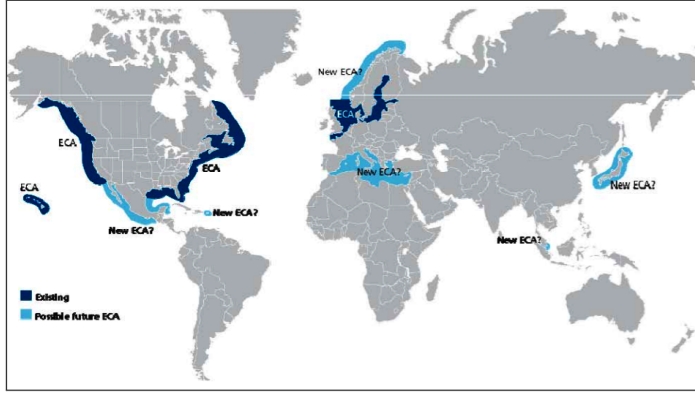


Figure 2.1: ECA and SECA areas (McGill et al. 2013).

2.1 EEDI and SEEMP

To fulfill rules IMO has developed global CO₂ reduction index known as Energy Efficient Design Index (EEDI). EEDI is based on ratio of total CO₂ emission per tonne-mile. CO₂ emissions depend of fuel consumption. Therefore CO₂ emissions can be reduced simply by reducing fuel consumption. Purpose of EEDI is to achieve a minimum energy efficient level for new ships. All new ships from January 1st 2013 have to fulfill the minimum criteria of EEDI (Heinänen 2013). EEDI is a requirement the design has to fulfill but is not suitable as a design optimization criterion and to evaluate technoeconomical merit of a ship (von Bock und Polach et al. 2014). Hasan (2011) studied the impact of EEDI on ship design and hydrodynamics. The study shows that for vessel designed for slow speeds (10-12 knots), it is better to have small ship dimensions to fulfill EEDI. The study states that speed and length of the vessel have the highest impact on EEDI.

To fulfill EEDI ship must realise

$$EEDI \leq (1 - X/100) \cdot \text{Reference line value} \quad (2.1)$$

Reference line value means the minimum EEDI calculated for similar reference ships. X is a reduction factor in percentage (IMO 2012b). The reduction factor increases gradually every five years depending on ship size and type by 0.1 or 0.05 units at time. It is decided that the reduction factor is 0.30 in year 2025, *i.e.*, ship energy efficiency should be increased 30 % in 12 years after adopting EEDI. (Heinänen 2013)

Restriction for attained EEDI operates essentially as a power ceiling for ships. If ship has a high open water speed, it is possible to reduce speed and thus to reduce power demand. This reduces also fuel consumption. Ice-classed ships must use higher power compared to open water vessels in order to proceed in ice. In the EEDI equation this handicap is

compensated with some ice-class correction factors. These factors should convert power and deadweight of an average ice-class ship to be the same as an average open water ship. Effect of the ice-class correction factor is largest for an average ice-class ship and thus any extra power beyond the minimum ice class requirement is penalized. This will force the designers to find energy efficient designs with a good ice performance (Riska 2014a). The idea of a double acting ship is to reduce the power demand and therefore it might be a suitable alternative to help designers to fulfill EEDI.

IMO has also noted an amendment of ship's energy efficiency that come into effect on January, 2013. This amendment requires each ship to keep on board a ship specific Ship Energy Efficiency Management Plan (SEEMP). The purpose of SEEMP is to establish a mechanism for a company to improve energy efficiency of the operation of the vessel. Ship specific SEEMP is linked to a broader corporate energy management policy for the company that owns, operates or controls the ship. (IMO 2012a)

2.2 Ways to improve fuel efficiency

Fuel efficiency of a ship can be improved by taking into account some variables. A good design of hull is crucial. A good hull form designed for operational area can reduce resistance and hence save huge amount of fuel and transport time. Fuel consumption reflects directly to emissions the ship makes. Equipment on board should be chosen wisely, *e.g.*, by installing a waste heat recovery (WHR) unit. It can decrease energy consumption and emissions of the vessel. Speaking of an ice-going vessel, waste heat could be used, *e.g.*, to prevent icing of deck equipment or heating crew areas.

A good knowledge of transit route is very important. Time and fuel can be saved when planning and studying the route beforehand. Also knowing the route conditions, the shipping becomes safer. It is particularly important for ice-going vessels to avoid the most severe conditions. Knowing the conditions on the route, needed power can be predicted quite realistic and hence a proper machinery for the vessel can be chosen.

Alternative fuels, *e.g.*, Liquid Natural Gas (LNG) or Marine Diesel Oil (MDO), to replace low-quality, low-price residual fuel referred to as Heavy Fuel Oil (HFO), might be answer to reduce emissions and fulfill rules and regulations. These days approximately 77 % of marine fuel consumption is of HFO. In long term focus alternative fuels might become cheaper to use for shipping and some harbors use already cheaper fees for ships that fulfill sulfur limits as an incentive. However, before, *e.g.*, LNG could be a leading fuel for shipping it should have a proper distribution network. An existing diesel engine ship would need a conversion to LNG and for economic reasons an LNG conversion generally requires that 30-40 % of operation is located within ECA areas. Otherwise capital investment would be

too heavy (McGill et al. 2013). Therefore the most economic solution for ships operating shorter times in ECA or SECA areas is using HFO outside of these areas and change to, *e.g.*, Marine Diesel Oil (MDO) when sailing in ECAs and SECAs. Hence MDO is a drop-in fuel so no changes to existing diesel engine is needed for using it instead of HFO.

Used fuel affects on the CO₂ emissions. The CO₂ emission effect is received by multiplying the consumed fuel by emission factor. The emission factors for different, usually ship used, fuels are listed in table 2.1. (Hippinen and Suomi 2012)

Table 2.1: Emission factors for different fuels.

Fuel	kgCO ₂ /MWh
Heavy fuel oil	284
Light fuel oil	261
Liquid gas	234
Natural gas	198

Reduction of NO_x, SO_x and CO₂ elements are sometimes competing against each other. As an example installing a wet scrubber and therefore achieving reduction of sulfur means increasing power usage significantly to pump water, which in the end will lead to an increase in CO₂ emissions. (McGill et al. 2013)

Chapter 3

State of the art for Northern Sea Route and transit-simulation studies

Suitability of the NSR for shipping between Europe and Asia has been studied from different points of view. Most studies have focused on the economics of shipping via the NSR. The fuel efficiency has not been studied much. In this chapter, state of the art is introduced. Every publication is presented briefly. The publications are divided into the ones that deal with the NSR and the ones dealing with transit-simulations. Publications are organized chronologically.

3.1 Northern Sea Route -studies

The most recent publications of the feasibility studies related to the NSR are:

- Verny and Grigentin (2009)
- Omre (2012)
- Erikstad and Ehlers (2012)
- Sørstrand (2012)
- Otsuka et al. (2013)
- von Bock und Polach et al. (2014)
- Schartmüller (2014)
- Way et al. (2015)

Verny and Grigentin (2009) study the relative costs of various axis in the Asia-Europe transport network, including the NSR. The result of the study is that it is still the least expensive to ship through the SCR. The NSR and Trans-Siberian Railway appear to be

roughly equivalent second-tier alternatives. However, this study was not done by the use of simulation method and therefore, *e.g.*, the specific ice conditions were not included.

Omre (2012) identifies an assesment framework to integrate the northern and southern passages together in an economically feasible transport system. The study takes into account route limitations and vessel restriction on the NSR. Feasibility of the transit route is evaluated with the required freight rate (RFR). The results of the study show that slow steaming is more profitable than increasing the transits a year. Also the NSR is more profitable option in quite light ice conditions for all ice classes.

Erikstad and Ehlers (2012) presented a decision-support model identifying the most viable ice class for a liner vessel transiting along the NSR. The model takes into account the time-dependent length of the NSR sailing season and corresponding roundtrip times, the additional capital expenditure and operational expenditure for ice class capabilities for the vessel and the fuel price. The results state that with longer time periods, allowing the NSR to be transited with lower ice classes, the choice of ice class 1A becomes most prominent, while the additional investment in 1AS is too high to be reimbursed and the gain due to 1C compared to no ice class is insignificant to justify its expenditure.

Sørstrand (2012) assess design aspects for vessels using the NSR in addition to the SCR. The study presents a decision support model to assess the potential financial benefit using the NSR. The study takes into account: ice conditions, ship parameters and her performance in ice, operational window on the NSR, initial investment cost of the vessel and the operational and voyage costs. The results shows that 1A ice class needs approximately 60 operational days on the NSR before profiting. Also the 1A vessel is profitable as long as there is less than approximately 1500 nm of ice on the NSR, and the fuel price higher than approximately 550 USD/ton.

Otsuka et al. (2013) presented the results of an investigation on the feasibility of shipping via the NSR with commercial voyage records. The conclusions of the study was that the shipping season starts in late June and continues through late November. The study made also a cost estimation for shipping of LNG through NSR and SCR, shipping iron ore using NSR and Panama Canal and shipping frozen fish via NSR and SCR. The results shows that the NSR is the most cost efficient solution for all above mentioned situations.

In their study von Bock und Polach et al. (2014) extended the ship merit factor (SMF) for ice-going vessels. The article presented a method that combines the SMF with a route specific ship-dependent productivity and allows to compare the technoeconomic performance of ships operating in open water and ice. One aim of the study was to examine, does an ice class increase the profitability, and if it does, which ice class should be selected.

The results of the study was that the overall performance of a vessel that sails via SCR is superior to the ice-classed vessels sailing the NSR. Also one conclusion was that an ice class does not increase profitability, but if the selection has to be made between the ice-classed ships, it would be the ship with higher ice class (in the case study Arc5 rather than Arc4 (Russian Register)) due to the better comparative ship merit factor (CSMF).

Schartmüller (2014) introduced a simulation-based decision-support tool to support stakeholders in the decision making process of integrating arctic routes in the transport system. The tool presented in the study has the capability to evaluate the economic feasibility of different route options and deal with the related uncertainties in input variables like climate development. The study takes into account charter costs, fuel costs, route fees and insurance costs. Results of the study indicate that the NSR is not competitive compared to the SCR with used ice data and assumptions made in the study, but has the potential to become a considerable option in economical view under certain conditions in the future.

Way et al. (2015) determine whether it is more profitable for a container shipping company to ship from Europe to Asia through the Suez Canal route (SCR) year-around or to use the Northern Sea Route (NSR) during the months it is passable while using the SCR for the remainder of the year. The study utilizes speed optimization as part of the economical analysis to find an optimal speed for shipping via different routes. The speed optimization is done due to its link with fuel consumption. The study takes into account fuel costs, capital costs, operating costs and transit fees. They found that it is somewhat more profitable to use the SCR.

3.2 Transit-simulation

Transit-simulation publications are listed below:

- La Prairie et al. (1995)
- Riska et al. (1997)
- Kotovirta et al. (2009)
- Guinness et al. (2014)
- Choi et al. (2015)

La Prairie et al. (1995) introduced a preliminary design tool used to approximate the suitability of various ships for transiting routes of various ice conditions. Suitability of a

ship is measured in terms of speed and energy expenditure, calculated with resistance formula developed mainly for the Baltic. Compared to other studies the program introduced in this publication includes also ridged ice.

Riska et al. (1997) presents the outcome of a study aimed at a better understanding of the factors influencing the resistance of a ship in a broken lead in the Northern Baltic. The study is based on observations of the performance of multiple ships in the ice during several winters. The study ends up with a proposal for a new method for determining the powering requirements in the Finnish-Swedish Ice Class Rules.

Kotovirta et al. (2009) introduce the Ice Ridging Information for Decision Making in Shipping Operations (IRIS) system prototype. The IRIS system combines state of the art ice modeling, ship transit modeling and optimization methods as an operative on board route optimization system prototype for ice-covered waters. The system takes into account the effect of level ice thickness, ridged ice thickness and ice concentration on the ship speed. The validation of the system was done within the Baltic Sea on board a merchant vessel. The comparison between the estimated transit time, with the IRIS system, and true transit time indicated that the error of the transit time estimate was below 7 %.

Guinness et al. (2014) present a method for ice-aware maritime route optimization. The aim of the study is to increase the safety and efficiency of maritime transport under icy conditions. The paper focuses on examples from the Baltic Sea. The study states that the route optimization algorithm can be used to minimize the costs associated with sailing through ice-covered waters.

Choi et al. (2015) presents a path planning problem in ice-covered waters as a dynamic stochastic path planning problem by generating a map through the ensemble simulation of an ice model.

3.3 Summary

Above described studies address various aspects of usage of the NSR. Most of the state of the art studies, dealing with the NSR, concentrates only on the economical point of view. In the simulations, fuel efficiency has been dealt only slightly.

Studies deal with the NSR only as part of the year option, *i.e.*, no study has taken into account a possibility for a ship to sail the whole year there. All the studies are done for ships escorted by an icebreaker in the NSR. Therefore the only resistance the ship encounters is due to brash and level ice. No study takes into consideration the double acting concept when the ship should be able to sail independently in ice covered areas. In

some of the studies quite realistic ice conditions on the NSR have been taken into account but solely the level ice conditions, *i.e.*, thickness and concentration and no ridge fields and their effect on the channel thickness.

There are publications addressed for transit-simulation and the route optimization. However, most of the studies concentrate on the Baltic Sea. This thesis will make an exception to that. Only La Prairie et al. (1995) uses method presented by Malmberg (1983) to study the resistance caused by ice ridges. Other one uses the method presented by Riska et al. (1997) where the ridge resistance is simplified. In this thesis the used ridge resistance method is the one presented by Malmberg (1983).

Chapter 4

Sea ice on the Northern Sea Route

When the weather cools down the surface layer of water is being cooled to densities that are higher than those of the underlying warmer fluid. This is an unstable situation that results in the development of convective mixing in the upper portion of the water column. As cooling continues convection also continues until the complete thickness of the convecting layer has been cooled to the freezing temperature and ice starts to form. This is valid only for salinity greater than 24.7 %. Typical sea water freezes at *ca.* -1.8 °C. Difference from fresh water freezing temperature, 0.0 °C, is due to salinity of sea water. The salinity varies and depends of the sea. Near-surface salinities in polar regions are typically in the 31-34 % range. (Weeks 2010)

Ice concentration is a measure of the mean areal density of ice in an area. Ice can be one-year or old ice, *i.e.*, having survived at least one melting season. Sea ice can appear in multiple forms such as level ice, ice floes, ice ridges, hummocks, rafted, etc. In this thesis ice conditions are limited to one-year ice which consists of level ice, ice channels and ridges. In this chapter these conditions are explained.

4.1 Ice conditions used in the thesis

The ice conditions used in this thesis can be found from appendix A. These conditions consists data from Arpiainen and Kiili (2006) for average and severe winter. The NSR is divided into 11 segments to get more realistic and varying conditions, figure 4.1. Ice conditions in the Kara East on April for both average and severe winter are presented in table 4.1 as an example.

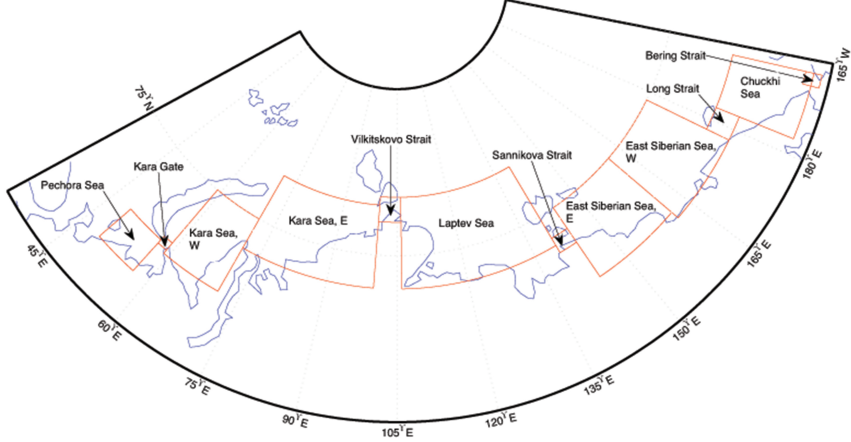


Figure 4.1: The NSR divided into segments.

Table 4.1: Ice conditions in the Laptev Sea on average and severe winter on April.

Variable	Average	Severe
Concentration [%]	98	98
Level ice thickness [m]	1.4	2.2
Mean ridge thickness [m]	10.0	10.0
Ridges per kilometre	5.0	7.0

To validate the used data they are compared to the data presented by Lensu et al. (1996). The comparison can be found from figures 4.2, 4.3, 4.6 and 4.7. From these figures can be seen that the ice data presented by Lensu et al. (1996) corresponds quite well to the average winter conditions presented by Arpiainen and Kiili (2006). The biggest difference between the data is in the ridge density, see figure 4.7, where Lensu et al. (1996) gives smaller densities in some areas, but mostly the densities correspond quite well. Note that the data presented by Lensu et al. (1996) does not contain conditions for Bering Strait, Kara Centre nor Kara Gate.

4.2 Level ice

The simplest measure for the ice conditions is the thickness of undeformed level ice (Riska et al. 1997). Kotovirta et al. (2009) states that if the concentration is below 70 % the ship is able to circum-navigate the floes and the ice. Therefore the performance is investigated with open-water characteristics. While simulating level ice conditions, the important factors are the thickness and flexural strength. In this thesis the flexural strength is assumed to be 500 kPa which is typical in Arctic Sea (Kujala and Riska 2010). The thickness depends on the month and the sea area and in this thesis it varies from 0 to 2.6 metres. The difference on level ice thickness, used in this thesis, can be seen in figures 4.2 and 4.3.

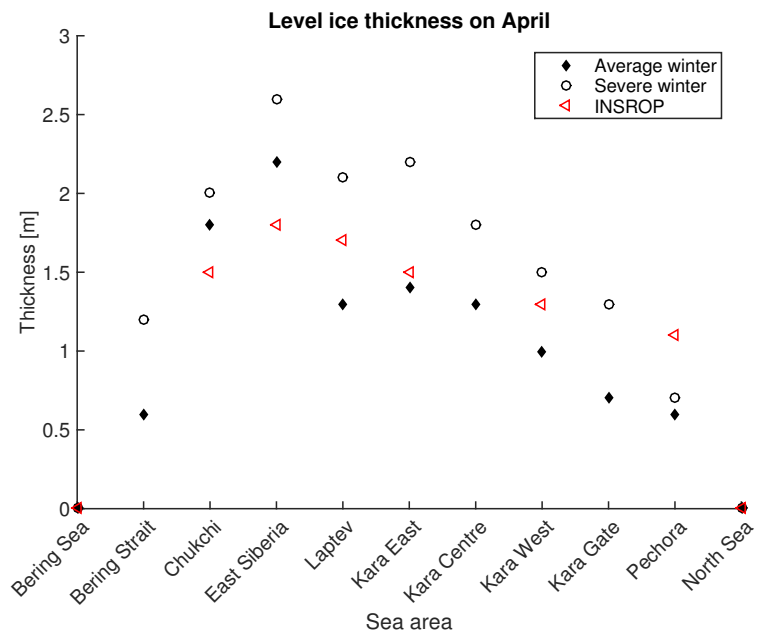


Figure 4.2: Level ice thickness on April for average and severe winters (INSROP means data from Lensu et al. (1996)).

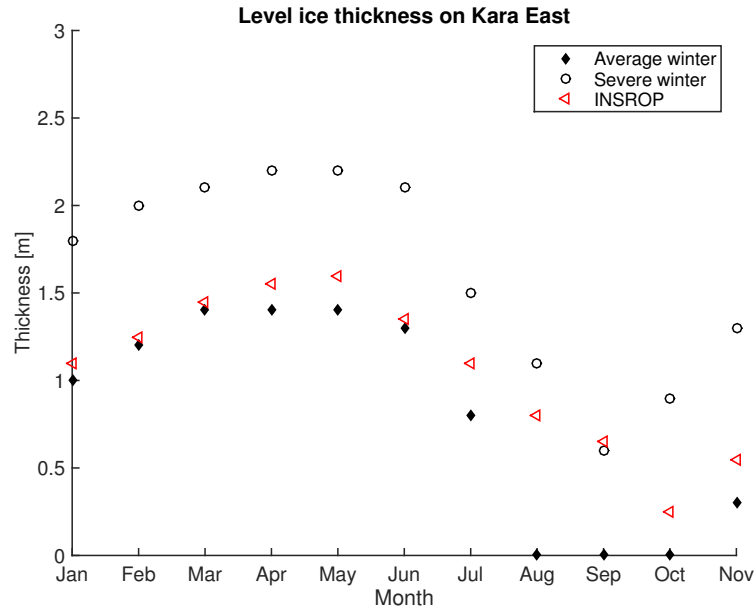


Figure 4.3: Level ice thickness in the Kara East for average and severe winters (INSROP means data from Lensu et al. (1996)).

4.3 Ice channel

An ice channel is made by a ship, *e.g.*, an icebreaker. It consists of ice pieces the breakage event forms, *i.e.*, brash ice. If it has been longer period since a ship has sailed through the channel, ice blocks start to freeze together, *i.e.*, a consolidated channel is formed. Consolidated layer resembles level ice. Channel resistance arises from displacing brash ice present in the channel both down and sideways (Riska et al. 1997). Usually a channel is thinner from middle compared to the sides (Kujala and Riska 2010). A typical ice channel can be seen in figure 4.4.

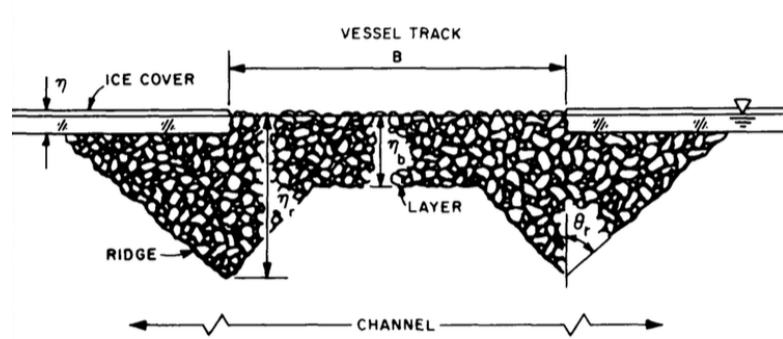


Figure 4.4: Profile of an ice channel (Ettema and Huang 1990).

If an old channel is navigated repeatedly the amount of brash ice increases due to the mixing of new ice and old brash. In this thesis the assumption is that vessels using the channel encounters only brash ice, *i.e.*, no consolidated layer, because they are always escorted by an icebreaker.

4.4 Ice ridge

An ice ridge is formed by compression or shear in the ice cover. Ice cover is broken, and due to the wind and currents a pile of broken ice, water, snow and air is created. The volume over water-line is called the sail. Below the waterline is the keel that contains most of the volume of the ridge. The keel is usually 5-7 times thicker than the sail (Kujala and Riska 2010). A typical ice ridge can be seen in figure 4.5.

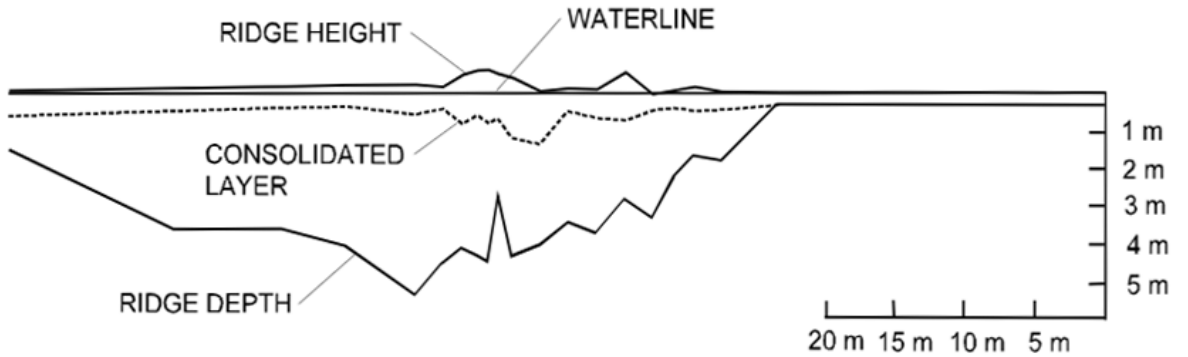


Figure 4.5: Profile of an ice ridge (Veitch et al. 1991).

In an ice ridge there are pores which are filled with water in the keel and air and snow in the sail. When water freezes up the porosity decreases. This creates a frozen zone that grows downward in the ridge, *i.e.*, ridge is consolidating (Høyland 2002). The consolidated layer resembles level ice which the ship has to break. However, thickness of this layer has noted to be 40-70 % thicker than the thickness of level ice surrounding the ridge (Kujala and Riska 2010), see figure 4.5. Therefore and due to the thickness of the ridge rubble, which can be greater than the draft of the vessel, a ridge is the most challenging for a ship to go through (Kujala and Riska 2010).

Ridges are complex structures with a wide variability in shape and size. They are often modeled by triangles or trapezes and characterized by their thickness, widths and angles (Strub-Klein and Sudom 2012). The maximum thickness of an ice ridge on the NSR is based on several measurements presented by Strub-Klein and Sudom (2012). The maximum thickness is 28 m. This value is used in this thesis as the maximum input on

simulations, see Chapter 8. In figures 4.6 and 4.7 can be seen the total ridge thickness, *i.e.* the sail plus the keel, and density, *i.e.*, number of ridges in one kilometre, on April on the NSR.

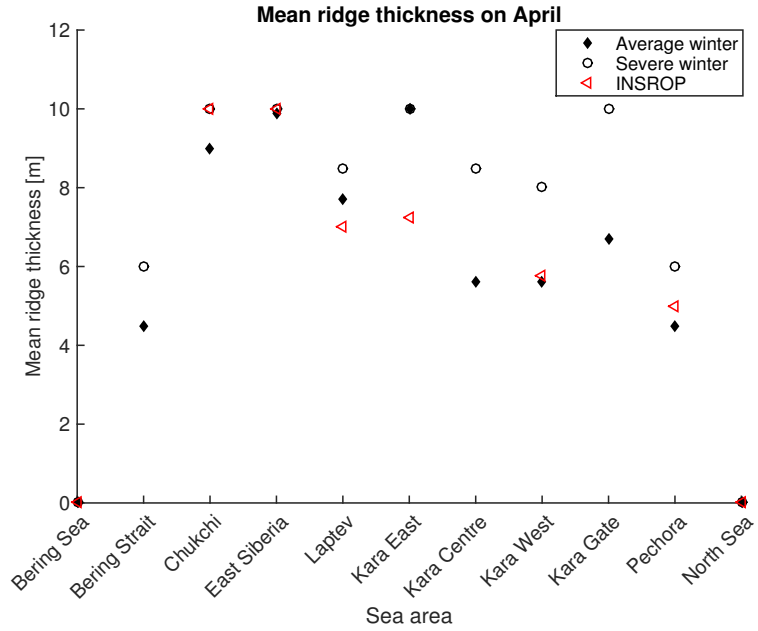


Figure 4.6: Ridge thickness on April (INSROP means data from Lensu et al. (1996)).

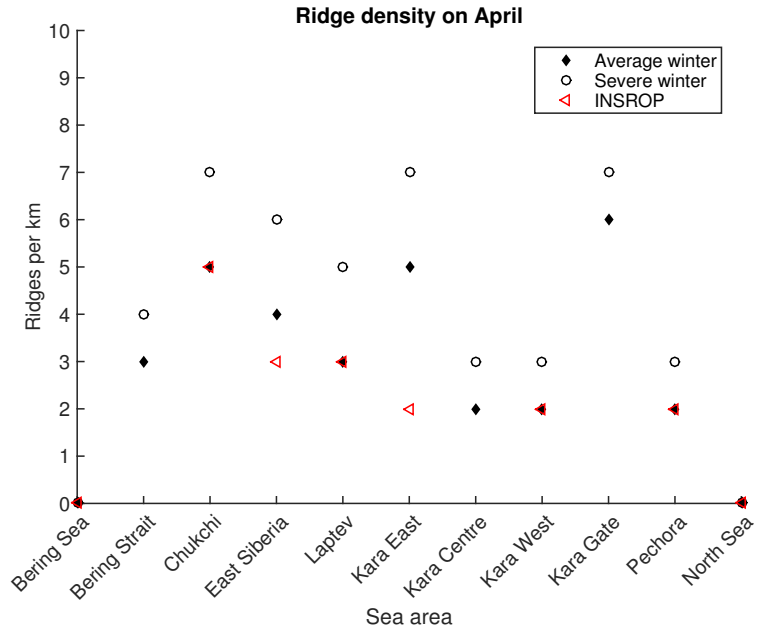


Figure 4.7: Ridge density on April (INSROP means data from Lensu et al. (1996)).

Chapter 5

Ice-going vessel characteristics

In this chapter, first icebreaking process is presented. After that the characteristics and design challenges of an ice-going vessel are described. Finally the double acting -concept is explained.

5.1 Icebreaking

The performance of an ice-going vessel is determined by how it proceeds in ice. This is usually measured with transit-times through ice-covered areas and the energy consumed in making the transit. Good performance in ice is characterised with low ice resistance, high propulsion efficiency and power resulting in high thrust. A capable and experienced crew operating in ice is also crucial. One of the most important characteristic for an ice-going vessel is that it does not get stuck in ice. (Riska et al. 1997)

Ice conditions can vary much during one trip - the vessel can encounter level ice, ice ridges, including long ridge fields, channel ice, pack ice and compressive ice. Ridged ice fields and compressive ice are very demanding conditions for a ship to operate. While penetrating a ridge, the ship breaks the consolidated layer in the same way as it breaks level ice, but the ice blocks piled in the ridge sail and keel must also be displaced. Ridge keel depths can exceed the ship draft and a lot of energy is consumed by submerging, clearing, and frictional resistance (Veitch et al. 2003). Presence of ice pieces at the propeller may seriously impair propulsive performance. Large ridges that cannot be penetrated by continuous icebreaking must be rammed or if possible circum-navigated. Effective ramming operations require high thrust at medium and low speeds (forward and astern) causing load changes to the machinery. These load changes cause increase in the fuel consumption. (Hänninen et al. 2012)

Different ice conditions set some limits also to the hull structures. Ships that navigate in ice are regulated according to the rules of various classification societies and regulatory

bodies. The hull structure must be strengthened locally to withstand very high local ice contact pressures. Also, the global hull girder must be of adequate strength to accommodate bending loads associated with ramming. The environmental ice conditions at the operational area are the basis of the class restrictions. (Veitch et al. 2003)

As a ship proceeds into an ice sheet, the ice edge is crushed at different locations distributed over the hull-ice contact interface. As penetration continues, the ice sheet is progressively deflected down as the hull slides over it. Local contact pressure between the ice and hull gives rise to friction during the submergence of the ice edge. Local ice failure at the contact area may continue during submergence. Bending of ice sheet results in its failure through flexural fracture. The piece of ice cracked off the sheet is then submerged under the moving hull and eventually reemerges and clears the ship. To break level ice effectively, the bow form should promote flexural failure of ice rather than crushing. (Veitch et al. 2003)

Icebreaking process can be seen from figures 5.1 and 5.2. Figure 5.1 shows the way the bow area breaks the ice; by crushing and bending. From figure 5.2 ice movement along the hull during the breaking process can be seen.

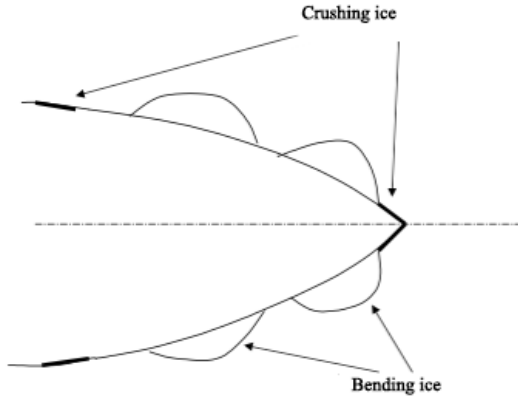


Figure 5.1: Ice breaking process of the bow area (Kujala and Riska 2010).

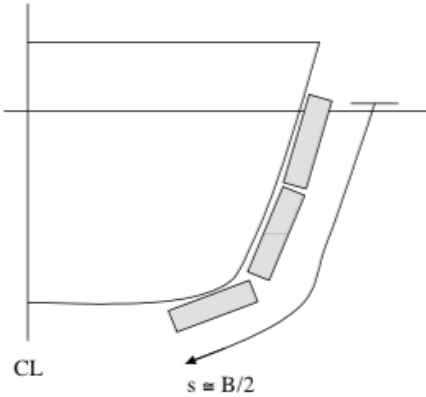


Figure 5.2: Ice movement along the ship hull (Kujala and Riska 2010).

Ice resistance refers to the time average of all longitudinal forces due to ice acting on the ship. These ice forces are divided into categories of different origin: breaking force, submergence force and sliding force. The relative importance of these components arises in different ice conditions. The breaking component is usually largest in level ice but in brash ice or in smaller ice floes the other two components become more important. Breaking force is related to the breaking of the ice, *i.e.*, to crushing, bending and turning the ice. Submergence is related to pushing ice down along the ship hull whereas the sliding forces include frictional forces. Usually the velocity dependance of the ice resistance is attributed to the last component. (Riska 2010a)

5.2 Designing basics

To design an ice-going vessel the designer must know where the ship is going to operate and what kind of operations the vessel is going to perform. The operations range from transportation to dedicated ice breaking and ice management roles. Designer needs knowledge on how ice is acting on the ship and how the interaction is modeled. A design for a ship operating in ice includes three aspects: ship structures must have an adequate strength to endure ice loads, performance of the ship must meet the functional requirements and ship systems and equipment must function in cold temperatures (the ship must be able to operate at least in a temperature of -35 °C). (Riska 2010b)

The choice of ice capabilities to be incorporated in the design of a merchant ship depends on the amount of time spent in ice-covered water relative to open water, ice conditions on the route and on availability and associated costs of icebreaker escort service on specific routes. For ships designed for independent ice navigation, ice has more fundamental impact on the design. The designer must pay attention to the operational requirements of these ship types. It gives an appreciation of the implications on the design, particularly with

regard to hull form, structure, powering and maneuvering and auxiliary systems. For ships operating mainly in ice covered waters ice breaking is the most obvious operational requirement. Typically an ice-breaking ship would be expected to make quite good speed, *i.e.*, 10 to 12 knots, in ice conditions considered the norm in its operational area. (Veitch et al. 2003)

Machinery and hull strength of an ice-going ship are mostly designed based on experience from earlier ships. When damage caused by ice has occurred, strengthening of the structures is indicated. These experiences have been collected into the rules of classification societies. Most of the strength design is done following these rules. (Riska 2010a)

Operations in open water of an ice-going vessel must be considered in the designing phase. With an icebreaking bow ice resistance is reduced, but simultaneously open water resistance is increased. There are multiple ways to reduce the resistance caused by ice-operations. A good low friction paint resists the abrasion of ice and reduces frictional resistance between ice and hull. Several other systems designed to reduce friction have been developed, *e.g.*, air bubbler systems that pump compressed air out of small nozzles in the hull at the midbody and bow. This system reduces frictional resistance. However, it is only effective at relatively low speed. One way to reduce ice-resistance is water deluge or water wash system. However, these systems require power that could be incorporated alternatively into the propulsion system. Heeling tanks are one way to aid icebreaking and increase maneuverability. (Veitch et al. 2003)

Choice of propulsion machinery for ice-capable ship is a compromise of multiple factors. It must be based on capital and operating costs, reliability, power to weight ratio and efficiency. Propulsion systems should be highly responsive for maneuvering and must be operated effectively even while subjected to repeated, intermittent, high torque loading due to propeller impacts with ice. Medium speed diesel engine is the most common prime mover used on ice-going ships. These have relatively good power to weight ratios and fuel consumption, use relatively inexpensive fuel and are compact and reliable. Best solution for ice-capable ships is a diesel-electric system. These cope better with ice torque loads by decreasing shaft speed compared to geared diesel engines. Flexibility in machinery arrangement is another advantage afforded by diesel-electric systems. (Veitch et al. 2003)

Diesel-electric machinery allows so called "*power plant principle*". It means the electric power and the propulsion power the ship needs are produced with the same machinery. With this solution fuel consumption can be reduced. This is possible because the load level of machinery can be optimized more freely with the number of used engines and loading rate. Placement of the diesel-electric system is more free and therefore it is suitable for a podded propulsion system. Needed electric power for ship operations can be produced with

bigger main engines which have smaller specific fuel consumption. This enables savings of 3-5 % in electric production. (Häkkinen 1993)

5.3 Double acting ship

A double acting ship (DAS) runs bow first in open water and light ice conditions, *e.g.*, ice channel or thin level ice. In heavy ice conditions it runs stern first. Idea of running an icebreaker with stern first is over 100 years old (Juurmaa et al. 2001). However, this concept was made feasible after the application of electric podded propulsion due to its great maneuverability. A double acting -concept makes independent navigation also in the most severe ice conditions possible, *i.e.*, no need for icebreaker support (Vocke et al. 2011).

In open water the DAS achieves better performance with the open water bow than it would with an icebreaking bow. In heavy ice conditions the ship turns around and attacks ice with stern designed for icebreaking. When running astern with propellers first, the flushing effect of the propellers lowers ice resistance by flushing ice floes backward and decreasing the water pressure under ice cover (Vocke et al. 2011). Thus a better overall performance and economic effect can be achieved. A pulling type propeller is a typical solution in double acting ship. However, propulsion efficiency is slightly lower compared to bow-first operation (Sasaki et al. 2002).

The effect of the DAS operation becomes particularly evident when operating in ridge fields. There the proper way of operation is to slowly move astern, giving the propellers time to destroy the ridge by chopping ice blocks with propeller blades. It is not recommended to ram stern first. Load changes to diesel engines should be avoided when turning the POD-unit. This is achieved by keeping the power constant. Frequent load changes to diesel engines will lead to increased fuel consumption and shorter time between overhauls for engines. (Hänninen et al. 2012)

Chapter 6

Modelled ship concepts

In this thesis, four different cases are studied and compared. The case-ships are:

- A DAS operating year-around on the Northern Sea Route (NSR) (DAS).
- A ship with an ice-bow operating year-around on the NSR (ice-bow ship).
- An open water vessel operating year-around on the Suez Canal route (SCR) (open water ship).
- A vessel that operates on the NSR, assisted by an icebreaker, from July until late November and rest of the year via the SCR (assisted ship).

All the vessels have same parameters. However, DAS and open water ship are equipped with a bulbous bow and ice-bow and assisted ships do not have a bulb. According to Matusiak (2010) a bulbous bow can reduce open water resistance 10-30 %. In this thesis the reduction of open water resistance for the bulbous bow is assumed to be 10 %.

Assumption is that DAS and ice-bow ship can operate independently on the NSR year-around. However, if they got stuck in ice on some segment, they are escorted through it by an icebreaker. These vessels sail through ice field that contains level ice and ice ridges. Assisted ship uses the NSR from July until late November and is escorted by an icebreaker through ice, *i.e.*, the ice conditions for this vessel is limited to channel without consolidated layer.

In figure 6.1 the side profile of simulated ship-types are presented. The main dimensions and angles can be found from table 6.1. Figure 6.2 clarifies some of the main parameters and angles.

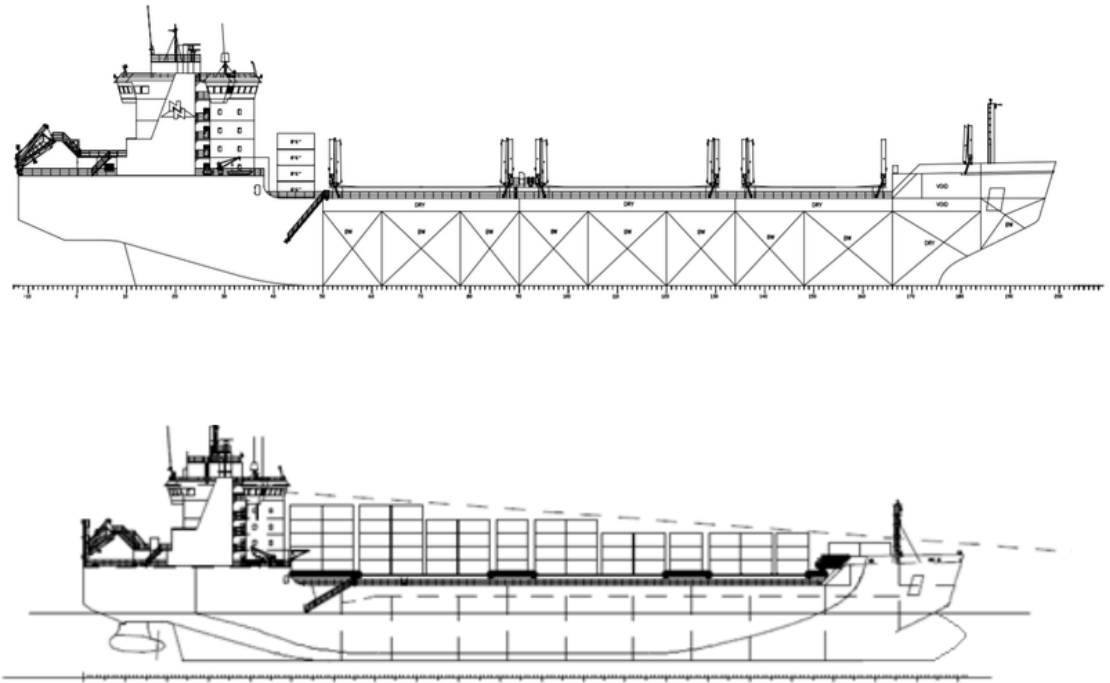


Figure 6.1: Above the side profile of a ship with an ice-bow and below the side profile of a typical double acting ship (Sillanpää and Mäkiranta 2014).

Table 6.1: Parameters for the case ships.

B	Breadth of the ship	23 m
C_m	Midship section coefficient	0.996
C_p	Prismatic coefficient	0.78
C_w	Waterplane area coefficient	0.961
L	Total length of the ship	170 m
L_{bow}	Length of the bow	37 m
L_{par}	Length of the parallel midship	100 m
L_{stern}	Length of the stern	33 m
L_{wl}	Length of the waterline	160 m
$P_{propulsion}$	Propulsion power	13 MW
T	Draft of the ship	9 m
α_{bow}	Waterline angle at the bow (see figure 6.2)	36.1°
α_{stern}	Waterline angle at the stern	38.9°
ϕ_{bow}	Stem angle at the bow (see figure 6.2)	22.3°
ϕ_{stern}	Stem angle at the stern	21.4°

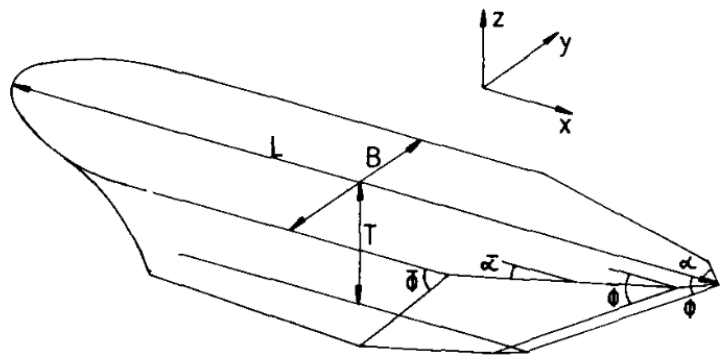


Figure 6.2: Definition of the main dimensions of a vessel (Lindqvist 1989).

Chapter 7

Investigated routes

Route used in this thesis goes from Rotterdam, Netherlands to city of Busan located in the southeast of South-Korea, see figure 7.1. In this chapter, this voyage is investigated through the Northern Sea Route and the Suez Canal route. These routes are described and compared. In the beginning of the chapter the importance of the route optimization is discussed.

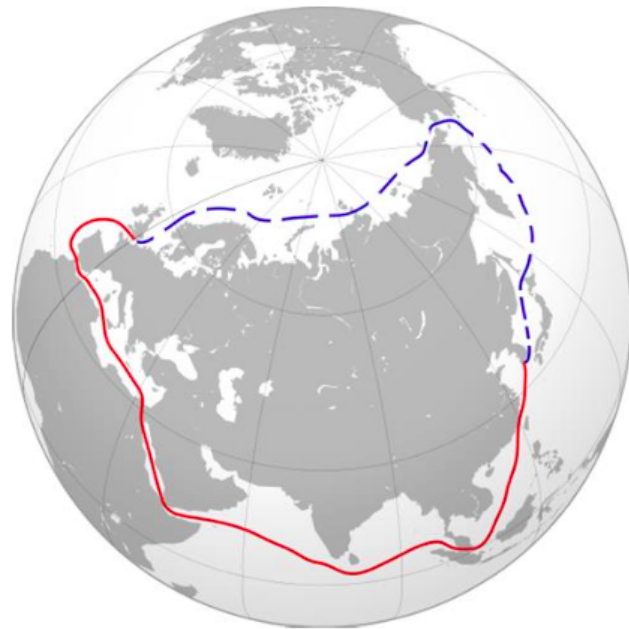


Figure 7.1: The Northern Sea Route (NSR) with blue and the Suez Canal route (SCR) with red (Way et al. 2015).

7.1 Route planning

A good plan and study of the route beforehand are crucial for a ship to sail safely and economically. Shipowner has to come up with the most economically efficient routes for the ship operations. The shortest route is not always the most economical one. It may be that it is also the toughest to operate - due to harsh ice or rough sea conditions. Route optimization should already begin in the design phase of the vessel. If the vessel has to be able to sail in ice covered areas it has to be ice strengthened to fulfill regulations and survive in ice conditions. It is not economically efficient to build a too strengthened ship with respect to encountered conditions.

For vessels traveling long distances in ice, it is worth planning routes that will reduce fuel consumption, travel time and the risk of getting stuck in the ice field or of ending up in dangerous areas. There is a multitude of information sources available for seafarers in ice-covered waters. For example near real-time delivery of satellite images to ice-going ships has been made for several years in different ice-covered sea areas like the Arctic. Computer-based optimization can be applied to ice routing, *i.e.*, selecting the best route alternative based on observed and predicted ice field properties. Ice models can be used to calculate predictions of the ice conditions surrounding the ship on its route to the destination. (Kotovirta et al. 2009)

Captain of the ship has to have good knowledge about the conditions of the route the ship is sailing. A captain of an ice-going vessel should have experience and knowledge of sailing in ice. Information about ice conditions can be found from ice charts. Knowledge and use of these charts are crucial for vessels operating in ice. Knowledge of past ice conditions and prediction of future ones are critical for a designer when designing an ice-capable ship.

Ice conditions are stored in a form of the World Meteorology Organization's (WMO) standard for ice charts, which is often referred to as "*Egg Code*", because of its shape, see figure 7.2. Different ice conditions can be determined from the Egg Code:

- Total (C_t) and partial (C_a, C_b, C_c) concentration of ice in a certain area
- Stage of development (S_a, S_b, S_c, S_o, S_d)
 - These can get values 1-9 and 1.,4.,7.,8. and 9., the values describe the thickness of the ice and tells if it is new or old, *e.g.*, 6 means first year (30 - 200 cm) (U.S. National Ice Center 2015)
- Predominant form of ice corresponding to the stage of development (F_a, F_b, F_c)
 - These can get values X, 0-9 and /, which describe what kind of ice it is, *e.g.*, 4 means medium ice floes (100 - 500 m) (U.S. National Ice Center 2015)

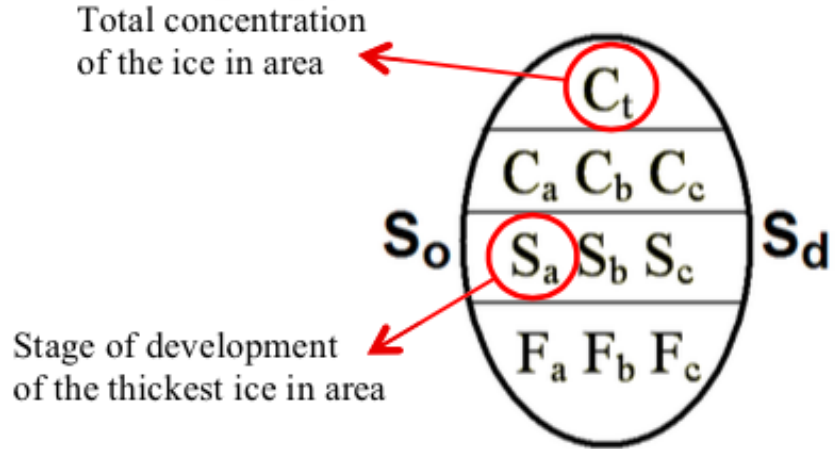


Figure 7.2: Egg Code (Tōns et al. 2014).

7.2 Northern Sea Route

Northern Sea Route is a historically existing Russian national transportation route. It is situated within a water area adjacent to the northern coast of the Russian Federation, covering the internal sea waters, the territorial sea and the exclusive economic zone of the Russian Federation, including tracks suitable for navigation. NSR is the shortest sea route between Northern Europe and East Asia. (Northern Sea Route Information Office 2015)

Ice conditions via the Northern Sea Route can vary much depending on the time of the year. Shipping season on the NSR starts in late June and continues through late November (Otsuka et al. 2013). The harshest conditions are between November and April (Way et al. 2015). Ice conditions in 2014 at the Arctic Sea can be seen in figures 7.3 and 7.4. Each image shows the concentration on the 15th of certain month. From these figures can be seen that from July until end of October the conditions are the lightest and lots of open water areas are along the NSR. Conditions in images 7.3 and 7.4 are quite close to the average winter used in this thesis what comes to the concentration.

Navigation via the Northern Sea Route is carried out in compliance with the Russian legislation, administrative procedures and international agreements of the Russian Federation (Northern Sea Route Information Office 2015). This is based on the principles of the UN Convention on the Law of the Sea, 1982, in particular article 234 *"Ice Covered Areas"*. (United Nations Convention on the Law of the Sea 1982)

The rules include, *e.g.*, that every vessel intending to navigate through the NSR shall obtain a permit from the Northern Sea Route Administration, the captain shall be experienced in operating a vessel in ice and obligatory requirements to have Civil Liability

Certificate. On the NSR the navigational period is determined by the Administration of the Northern Sea Route, vessel shall keep tracks recommended by the Marine Operations Headquarters (MOH) and in certain areas icebreaking guiding is mandatory. Design criterias ordains that a vessel must be ice classed. Selected ice class ordain the operation period and the areas where icebreaker guiding is mandatory (Balmasov 2013). In this thesis the ice class is Arc4 and hence the period for assisted ship using the NSR is from July until late November. A transit notice to navigate on the NSR has to be sent at least 4 months in advance (Omre 2012) and the fee depends of the need for icebreaker assistance (Northern Sea Route Information Office 2015).

Due to the rules on the NSR a ship would not be able to use it year-around. However, DAS and ice-bow ship using the NSR, is studied in this thesis to see if a ship could use it independently year-around. Also the rules may change in the future. A study about the DAS-concept is carried out, also due to the fact that it can be justifiable on operations in other ice covered sea areas.



Figure 7.3: Ice concentration on the Arctic Sea on January until June 2014 (Northern Sea Route Information Office 2015). In the figure on uppermost left the NSR is expressed with red color.

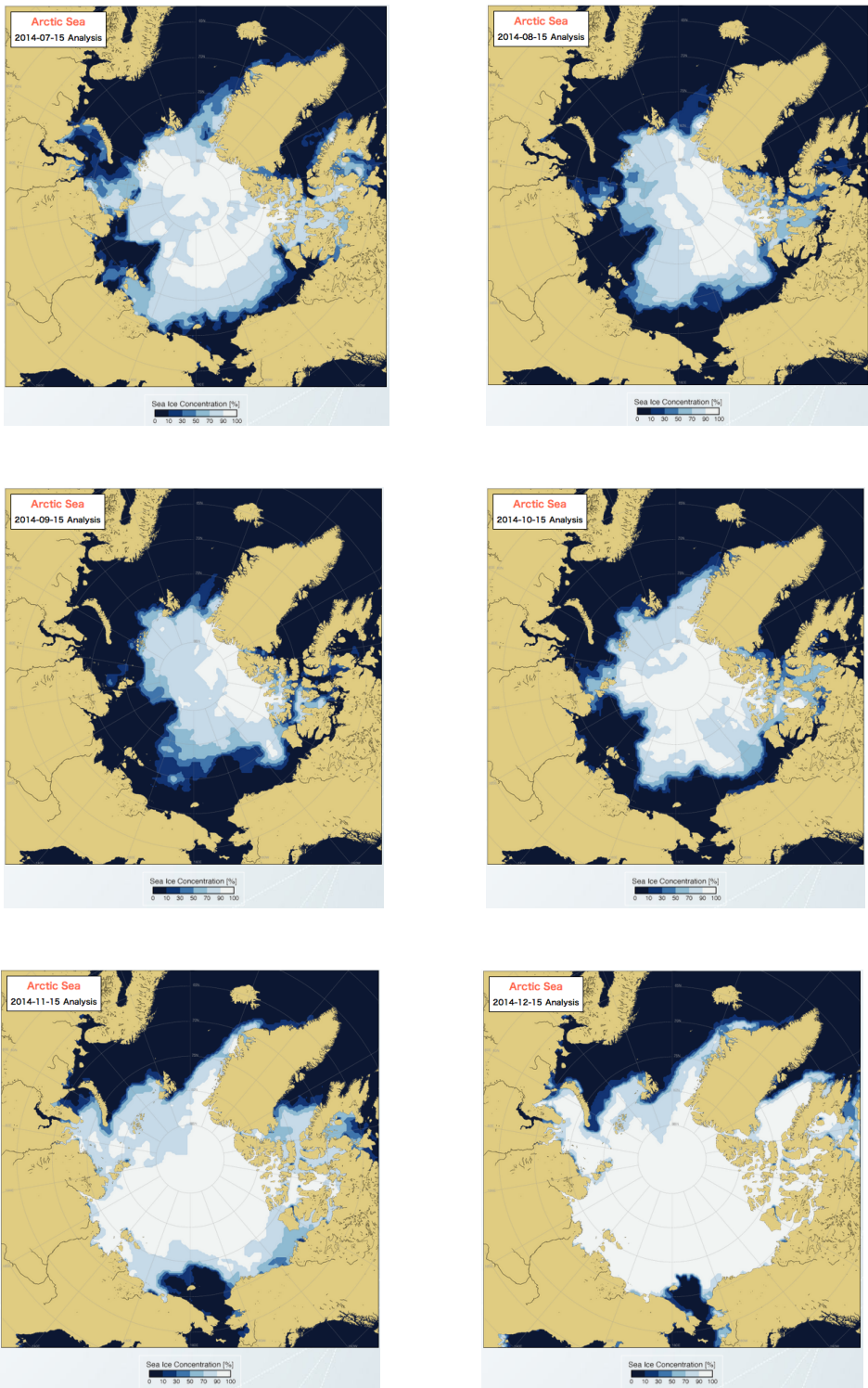


Figure 7.4: Ice concentration on the Arctic Sea on July until December 2014 (Northern Sea Route Information Office 2015).

7.3 Suez Canal route

Open water route connecting Europe to Asia goes along the Atlantic, Mediterranean Sea, the Suez Canal, Red Sea, Gulf of Aden, Arabian Sea, Indian Ocean, Malacca Strait, Singapore Strait, South China Sea and East China Sea. This route is known as the Suez Canal route (SCR). The bottleneck of the route is the Suez Canal which is located in Egypt and is 163 km long, figure 7.5. The canal connects the Mediterranean Sea with the Gulf of Suez. It has long been a link connecting Europe to South Asia. (Briney 2015)



Figure 7.5: The Suez Canal showed with the red line (Google maps).

Most of the canal is limited to a single lane of traffic. The vessels pass through in convoys and for joining a certain convoy the ship has to send an arrival notice at least 48 hours in advance. The fee of using the Suez Canal is based on the tonnage of the vessel, where the fees decrease per ton with increasing tonnage. The Suez Canal Authority has made a model to calculate the fee. The size restrictions in the canal are mainly the draft and the height of the ship. (Omre 2012)

In table 7.1 the characteristics of the NSR and the SCR are gathered.

Table 7.1: Characteristics of the routes.

	NSR	SCR
Length [km]	13 150	20 400
Max breadth	32 m	50 m
Max draft	13 m	20.1 m
Route fees	Depends on icebreaker need	Depends on net tonnage
Transit notice	4 months	48 hours

Chapter 8

Modelling methods

In this chapter, models to solve fuel and economic efficiency are presented. First the methods to generate the ridge field used in the simulations are presented. That is followed by the introduction of the used simulation methods and finally the models to solve the efficiencies are presented.

In the cases in which the vessel operates in either open water or in an ice channel, the speed of the vessel is assumed to be constant. Then, the propulsion power required to overcome the open water resistance or the ice channel resistance, respectively, is solved. In these cases speed of the vessel is expected to be 8.5 m/s in open water and 4 m/s in channel, which is a typical escort speed for 1A ice-classed vessel (Riska 2014b). For DAS and ice-bow ship the speed is solved in dominant ice conditions. Assumption is that DAS uses full power in ice, but also the performance with 80 % of full propulsion power is investigated to see if the vessel is able to use slow-steaming and how it affects to the fuel and economic efficiency.

8.1 Generating the ice field

In the transit simulations, the ice conditions are approximated as realistically as possible. The used ice conditions for two different winters, average and severe, can be found from appendix A. A ridge generator presented by La Prairie et al. (1995) is used for modelling the ridge field. Input data for the generator is ridge density per kilometre, *i.e.*, the amount of ridges on one kilometre on the segment, mean ridge thickness, keel angle and the maximum thickness of the ridges. With given input data the generator generates a ridge field containing random number of ridges. After multiple simulations the number of ridges corresponds to the ridge density given as an input to the generator. In transit-simulation the ridge generator is run 100 times, for simulating DAS, ice-bow ship and the assisted ship, to get a good sample of different ice fields and to eliminate incoherences.

The generator uses an exponential distribution in finding the ridge spacing (La Prairie et al. 1995).

$$p(x) = 1 - \exp(-\mu_s x) \quad (8.1)$$

This can be rearranged to find the position of the ridges.

$$x = (-1/\mu_s) \ln(1 - p(x)) \quad (8.2)$$

The variables of the equation (8.2) are given in table 8.1.

Table 8.1: Variables of equation (8.2).

Variable	Description
$p(x)$	Uniformly distributed
x	Distance between two ridges
μ_s	Expected number of ridges per kilometre

Ridge thickness can be found by

$$H_r = (-H_{keel}) \cdot \ln(1 - P(1 - p(x))) \quad (8.3)$$

The variables of the equation (8.3) are given in table 8.2.

Table 8.2: Variables of equation (8.3).

Variable	Description
H_{keel}	Expected keel depth
H_r	Ridge depth
$p(x)$	Uniformly distributed

After the thickness of the ridge is known the length can be solved with basic trigonometry by assuming the shape to be triangular.

$$x = \frac{H_r}{\tan(\kappa)} \quad (8.4)$$

Where κ is the keel angle of the ridge.

In figure 8.1 the output of four generated ridge fields, with the method by La Prairie et al. (1995) can be seen. All these four fields have the same input data, which can be seen in table 8.4. As can be seen from the figure the field contains different number of ridges with different distribution. Note that there also can be multiple ridges clustered.

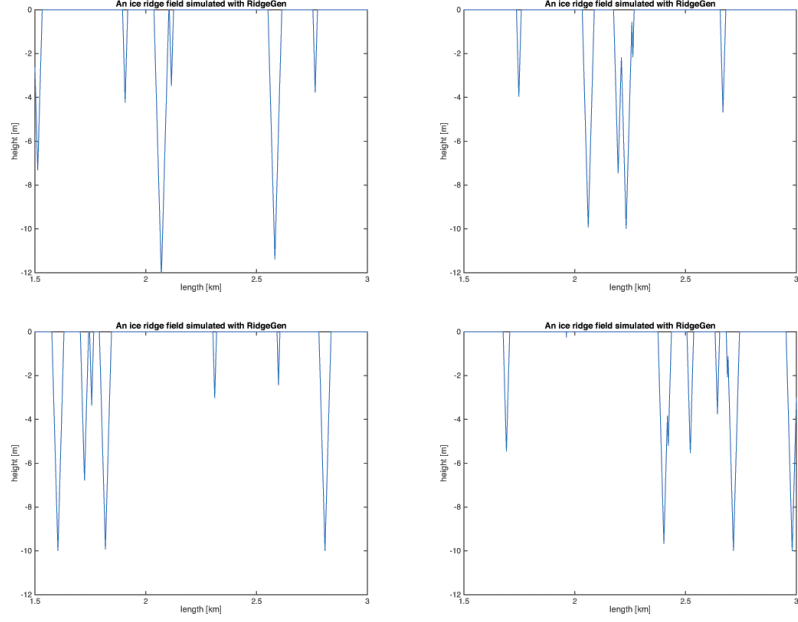


Figure 8.1: Four simulated ridge fields with same input parameters.

For comparison the ridge field is modeled with method presented by Kotovirta et al. (2009). This method flattens ridges, *i.e.*, total ice field consists of level ice and ridged ice, see figure 8.2. This method does not take into account the consolidated layer of the ridge. Equivalent thickness of the ridged rubble can be solved with equation

$$h_{eq} = 0.001 \cdot \mu_s \cdot \frac{1}{\tan \kappa} H_r^2 \quad (8.5)$$

The variables of the equation (8.5) are given in table 8.3.

Table 8.3: Variables of equation (8.5).

Variable	Description
h_{eq}	Equivalent ridged ice thickness
H_r	Average ridge thickness
κ	Keel angle (20°)
μ_s	Expected number of ridges per metre

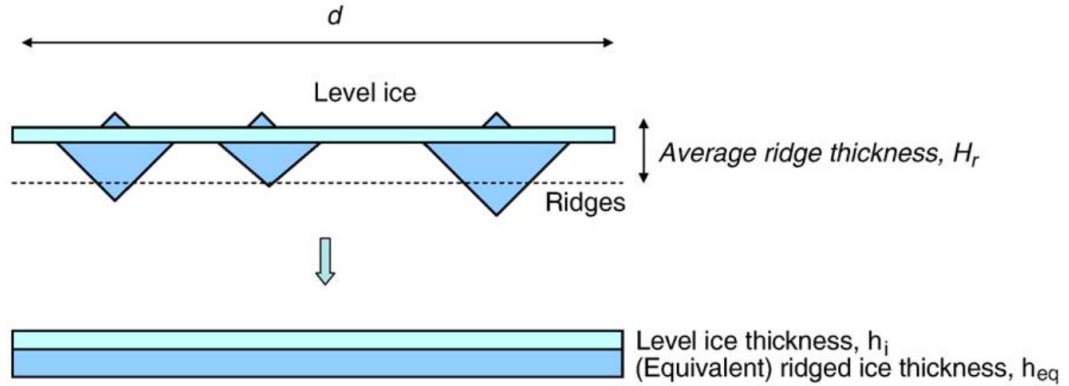


Figure 8.2: Above the ice field with triangular ridges. Under the ridge field as Kotovirta et al. (2009) models it.

These two ridge generating methods are compared to see how they relate to each others. If the relation is good much time can be saved by using the method by Kotovirta et al. (2009) for simulation. The difference of the output of these two methods can be seen from figure 8.3. From the figure, the difference with same input parameters can be seen. All of these ice fields has same input parameters, *i.e.*, mean keel thickness, ridge density and keel angle on the chosen segment. The input parameters can be found from table 8.4.

Table 8.4: Input data for ridge generator to generate fields in figures 8.1 and 8.3.

Variable	
Keel angle	20°
Maximum thickness of the ridge	28 m
Mean ridge thickness	7 m
Ridge density per km	4

In all generated fields the keel angle and the maximum ridge thickness are constant. Keel angle is assumed to be 20° (La Prairie et al. 1995) and the maximum thickness 28 m (Strub-Klein and Sudom 2012).

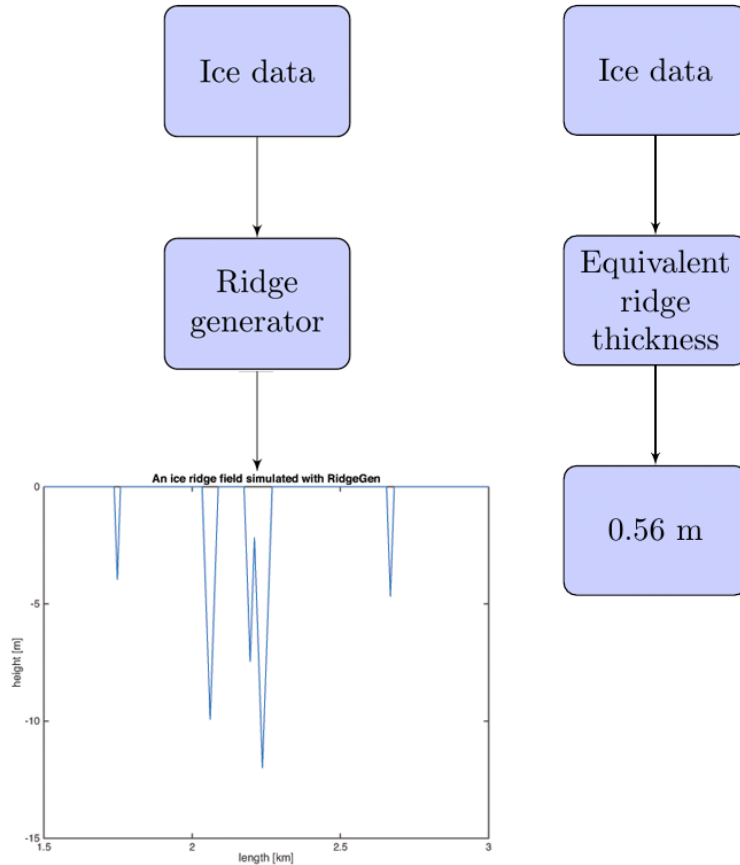


Figure 8.3: The flow charts of the two ice field generation methods. On the left the method presented by La Prairie et al. (1995) and on the right the method by Kotovirta et al. (2009).

8.2 Transit-simulation

With transit-simulation the ship progress in realistic ice conditions can be modeled. The purpose of the simulation is to study operational performance of a vessel on certain route. To get more accurate results of the simulation the route is divided into different segments with varying ice conditions. In this case, the route along the NSR is divided into 11 segments (see figure 4.1). The output of the transit-simulation is vessel speed for each segment for DAS and ice-bow ship. For open water and assisted ship the output is the power demand.

When power and speed is known the fuel consumption can be calculated with specific fuel consumption (SFOC) found from machinery handbooks. Input of the simulation is resistance equations in different ice conditions, *i.e.*, level ice without compression, channel and ice ridge. From figure 8.4 can be seen the flowchart of the simulations.

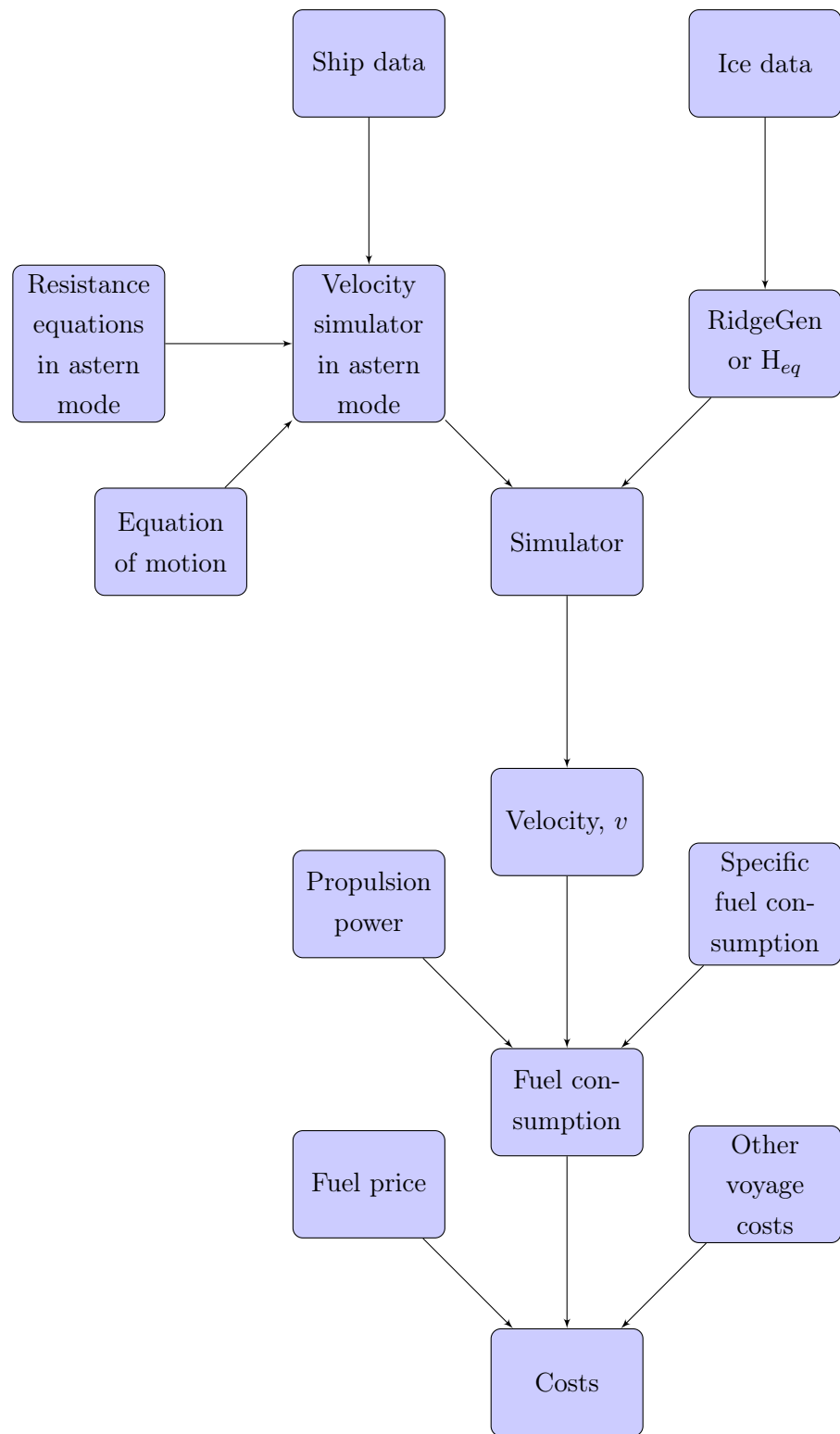


Figure 8.4: Flowchart of the simulation to get the fuel and economic efficiencies.

There are ways to solve the resistance the compressive ice field causes to a ship presented by Kaups (2011). However, taking into account the scope of this thesis and the accuracy of the method, the ice conditions are limited to level ice, ice channel and ridge conditions. Level ice is easiest to describe and resistance in level ice is the basis of all other ice resistance formulations (Riska 2010a). In this thesis channel ice resistance is only used to estimate the performance of the vessel escorted by an icebreaker, *i.e.*, channel without a consolidated layer. All of the ships investigated in this thesis has to sail also in open water conditions and the power demand is solved with help of the open water resistance equation. Next these resistance equations are presented.

8.2.1 Resistance equations

Level ice resistance

Level ice resistance is calculated with the method of Lindqvist. This resistance is divided into three components, *i.e.*, the breaking component R_b , crushing component R_c and the submergence component R_s . Then, the total resistance in level ice may be written as a linear combination of these (Lindqvist 1989).

$$R_{ice}^{Lindqvist} = (R_c + R_b)(1 + 1.4 \cdot Fn_{H_{ice}}) + R_s(1 + 9.4 \cdot Fn) \quad (8.6)$$

where Fn is the Froude number. Each component is written as

$$R_c = 0.5\sigma_b H_{ice}^2 \left(\frac{\tan \phi + \frac{\mu_H \cos \phi}{\cos \psi}}{1 - \frac{1 - \mu_H \sin \phi}{\cos \phi}} \right) \quad (8.7)$$

$$R_b = 0.003\sigma_b B(H_{ice})^{3/2} \left(\tan \phi + \frac{\mu_H \cos \phi}{\sin \alpha \cos \psi} \right) \left(1 + \frac{1}{\cos \psi} \right) \quad (8.8)$$

$$\begin{aligned} R_s &= (\rho_{water} - \rho_{ice})gH_{ice}B \\ &\times \left[\frac{T(T+B)}{2T+B} \right. \\ &\left. + \mu_H \left(\textcolor{red}{0.70}L - \frac{T}{\tan \phi} - \frac{B}{4\tan \alpha} + T \cos \phi \cos \psi \sqrt{\frac{1}{\sin^2 \phi} + \frac{1}{\tan^2 \alpha}} \right) \right] \end{aligned} \quad (8.9)$$

Variables of equations (8.6), (8.7), (8.8) and (8.9) are presented in table 8.5.

Table 8.5: Variables of equations (8.6), (8.8), (8.7) and (8.9).

Variable	Description
B	Ship breadth
H_{ice}	Ice thickness
Fn	$\frac{v}{\sqrt{gL_{wl}}}$
$Fn_{H_{ice}}$	$\frac{v}{\sqrt{gH_{ice}}}$
L	Ship length
T	Ship draft
α	Waterline angle (see figure 6.2)
μ_H	Coefficient of dynamic friction between the ship hull and ice
ρ_{ice}	Ice density
ρ_{water}	Water density
σ_b	Ice bending strength
ϕ	Stem angle (see figure 6.2)
ψ	$\text{Arctan}(\tan \phi / \sin \alpha)$

Equation (8.6) is validated for bow-first mode. Based on Tan et al. (2014) in astern mode the only difference is the area underneath the hull covered by broken ice and therefore the submerged part is

$$R_{sA} = (\rho_{water} - \rho_{ice})gH_{ice}B \times \left[\frac{T(T + B)}{2T + B} + \mu_H \left(\textcolor{red}{0.32}L - \frac{T}{\tan \phi} - \frac{B}{4 \tan \alpha} + T \cos \phi \cos \psi \sqrt{\frac{1}{\sin^2 \phi} + \frac{1}{\tan^2 \alpha}} \right) \right] \quad (8.10)$$

However, this should be considered critically due to the fact that it is based only on one model test series presented by Leiviskä (2004). The coefficients 0.70 and 0.32 in equations (8.9) and (8.10) mean the amount of ice going under the bottom of the vessel as a result of submergence, *i.e.*, ice covered area of the bottom. This coefficient is smaller in astern mode due to the flushing effect of the propellers. Ice underneath the vessel causes a friction force because it "pushes" the bottom of the vessel, due the lower density of ice compared to water (Kujala and Riska 2010).

The method of Lindqvist is validated for icebreakers without parallel midbody (Lindqvist 1989). The ships dealt with in this thesis are classical cargo ships and therefore they have

a parallel midbody. Despite of that the Lindqvist method is used due that it has been used earlier with good results in similar studies.

Ridge resistance

Ice ridge is the most complex in terms of resistance calculation and geometrical description and provides the greatest resistance to navigation along ice covered routes (La Prairie et al. 1995). Malmberg (1983) introduced a way to solve the ridge resistance

$$R_{ridge} = R_{bow} + R_{par} \quad (8.11)$$

In the formula of Malmberg the ridge resistance is a combination of resistance at the bow, resistance on the parallel midbody sides and resistance on the parallel midbody bottom.

The formula for bow resistance in an ice ridge is

$$R_{bow} = C_1 \cdot T \cdot H \cdot (B/2 + H \cdot \tan \phi \cdot \cos \alpha) \cdot (0.15 \cdot \cos \alpha + \sin \phi \cdot \sin \alpha) \quad (8.12)$$

The parallel midbody resistance, for sides and bottom, is

$$R_{par} = C_2 \cdot T \cdot L_{par} \cdot (0.27 \cdot H + (H/T - 0.5) \cdot B) \quad (8.13)$$

In equation (8.13) H is the ridge depth beneath a point along the ship at any moment. It can be considered $H(x)$, where x is the distance the ship has travelled across the ridge width. This can be determined by integration when the ridge profile is known. (La Prairie et al. 1995)

Simulating the ridge resistance with the method by Kotovirta et al. (2009) ridge thickness, H , in equations (8.12) and (8.13) is the equivalent thickness solved with equation (8.5).

Variables of equations (8.12) and (8.13) can be seen in table 8.6.

Table 8.6: Variables of equations (8.12) and (8.13).

Variable	Description
B	Ship breadth
C_1	Constant based on soil mechanics, 7500
C_2	Constant based on soil mechanics, 170
$H(x)$	Ridge depth beneath a point along the ship at any moment
L_{par}	Ship's parallel midbody region length
T	Ship draft
α	Waterline angle (see figure 6.2)
ϕ	Stem angle (see figure 6.2)

Equation (8.11) does not take into account the consolidated layer resistance. The formula of Lindqvist (equation (8.6)) is added to get the total resistance caused by the ice ridge. According to Kujala and Riska (2010) thickness of the consolidated layer is about 1.5 times the surrounding level ice thickness. Hence the resistance caused by ridge becomes

$$R_{ridge} = R_{ice}^{Lindqvist} + R_{bow} + R_{par} \quad (8.14)$$

Equation (8.14) is valid for bow-first mode. The effect of the stern-first operation in ice ridge has not been studied in publications. Therefore the author of this thesis has to find a valid method to analyse the ridge resistance in astern mode.

The effect of the stern-first operation in ice ridges was found with help of the level ice resistance equation in astern-mode. An assumption is that the astern-mode affects only to the bow resistance, R_{bow} , while penetrating through a ridge. The R_{bow} denotes the part of the resistance caused by the part of the ship that attacks the ice first, *i.e.*, stern in astern-mode. Hence equation (8.12) is multiplied with coefficient 0.77, later on called C_{AR} . This is worked out by dividing the submerged part of the Lindqvist equation in astern-mode, R_{sA} , by the one in bow-first mode, R_s , see equations (8.10) and (8.9).

$$C_{AR} = \frac{R_{sA}}{R_s} \quad (8.15)$$

As can be seen from equation (8.15) this coefficient is dependent on the ship parameters. The parameters of the case vessel is used to get the coefficient used in this thesis, *i.e.*, 0.77. These parameters can be found from table 6.1. Therefore the ridge resistance equation becomes

$$R_{ridge} = R_{ice}^{Lindqvist} + C_{AR} \cdot R_{bow} + R_{par} \quad (8.16)$$

8.2.2 Channel resistance

Channel resistance consists of two parts, one due to brash ice and one due to breaking the consolidated layer which has developed on the brash ice. The consolidated layer is absent when the ship is escorted or the channel is operated regularly. The resistance caused by brash ice is usually studied using soil mechanics. Riska et al. (1997) introduced a formula with speed dependence for brash ice resistance.

$$\begin{aligned} R_{ch} = & \frac{1}{2} \mu_B (\rho_w - \rho_i) g H_F^2 K_p \left[\frac{1}{2} + \frac{H_M}{2H_F} \right]^2 \left[B + 2H_F \left(\cos \delta - \frac{1}{\tan \psi} \right) \right] \\ & (\mu_H \cos \phi + \sin \psi \sin \alpha) + (1-p)(\rho_w - \rho_i) g K_0 \mu_H L_{par} H_F^2 \\ & + (\rho_w - \rho_i) g \left[\frac{LT}{B^2} \right]^3 \cdot H_M A_{WF} F n^2 \end{aligned} \quad (8.17)$$

Variables of equation (8.17) are presented in table 8.7.

Table 8.7: Variables of equation (8.17).

Variable	Description
A_{WF}	Waterline area of the foreship
Fn	The Froude number
g	Gravitational constant
H_F	Thickness of the brash ice layer which is displaced by the bow and which moves to the side against the parallel midbody
H_M	Thickness of the brash ice in the middle of the channel
K_0	Coefficient of lateral stress at rest
K_p	Coefficient of passive stress (soil mechanics)
L_{par}	Length of the parallel midbody at the waterline
δ	Slope angle of the side wall of the brash ice (in this thesis 22.6°)
μ_B	0.8 used in the thesis
μ_H	Coefficient of friction between the ice and the hull
ϕ	Stem angle

Thickness of the brash ice layer which is displaced by the bow and which moves to the side against the parallel midbody can be solved with equation

$$H_F = H_M + \frac{B}{2} \cdot \tan \gamma + (\tan \gamma + \tan \delta) \cdot \sqrt{\frac{B \cdot [H_M + \frac{B}{4} \cdot \tan \gamma]}{\tan \gamma + \tan \delta}} \quad (8.18)$$

In figure 8.5 the angles in equation (8.18) is shown.

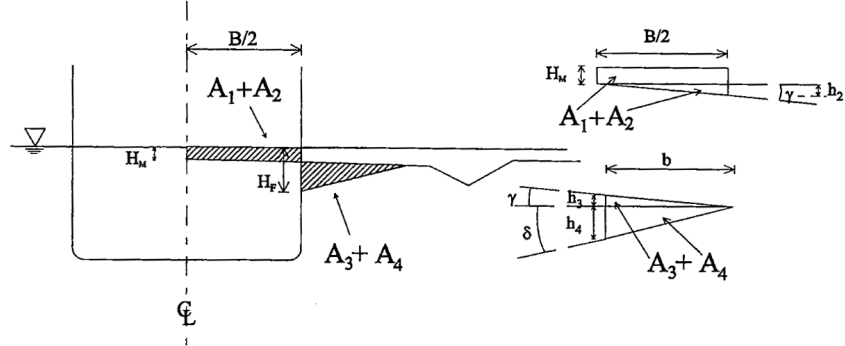


Figure 8.5: H_F angles (Riska et al. 1997).

Coefficients K_p and K_0 are calculated according to

$$K_p = \frac{1 + \sin \Phi}{1 - \sin \Phi} \quad (8.19)$$

$$K_0 = \frac{\nu}{1 - \nu} \quad (8.20)$$

Where ν is Poisson's ratio and for ice it is 0.33.

The resistance is very sensitive to the internal friction angle Φ . According to Kujala and Riska (2010) Φ varies from 42° to 58° . In this thesis 50° is used for the size of this angle.

The above described channel resistance is valid for bow-first operations. However, in this thesis the assumption is that if the DAS needs icebreaker assistance, it follows the icebreaker stern first. Therefore the coefficient C_{AR} , see equation (8.15), is used to multiply the part of the channel resistance where the hull shape has been taken into account. Therefore the channel resistance in aster-mode becomes

$$\begin{aligned} R_{chA} = & C_{AR} \cdot \frac{1}{2} \mu_B (\rho_w - \rho_i) g H_F^2 K_p \left[\frac{1}{2} + \frac{H_M}{2H_F} \right]^2 \left[B + 2H_F \left(\cos \delta - \frac{1}{\tan \psi} \right) \right] \\ & (\mu_H \cos \phi + \sin \psi \sin \alpha) + (1-p)(\rho_w - \rho_i) g K_0 \mu_H L_{par} H_F^2 \\ & + (\rho_w - \rho_i) g \left[\frac{LT}{B^2} \right]^3 \cdot H_M A_{WFF} n^2 \end{aligned} \quad (8.21)$$

8.2.3 Open water resistance

Open water resistance can be calculated with equation presented by Holtrop and Mennen (1982) and Holtrop (1984). This method is developed through a regression analysis of random model experiments and full-scale data. This method uses ship parameters as input data, see table 6.1. In figure 8.6 the effect of the speed to the resistance can be seen.

$$R_{total} = R_F(1 + k_1) + R_{APP} + R_W + R_B + R_{TR} + R_A \quad (8.22)$$

Variables of equation (8.22) is presented in table 8.8.

Table 8.8: Variables of equation (8.22).

Variable	Description
$1 + k_1$	Form factor describing the viscous resistance of the hull form in relation to R_F
R_A	Model-ship correlation resistance
R_{APP}	Resistance of appendages
R_B	Additional pressure resistance of bulbous bow near the water surface
R_F	Frictional resistance according to the ITTC-1957 friction formula
R_{TR}	Additional pressure resistance of immersed transom stern
R_W	Wave-making and wave-breaking resistance

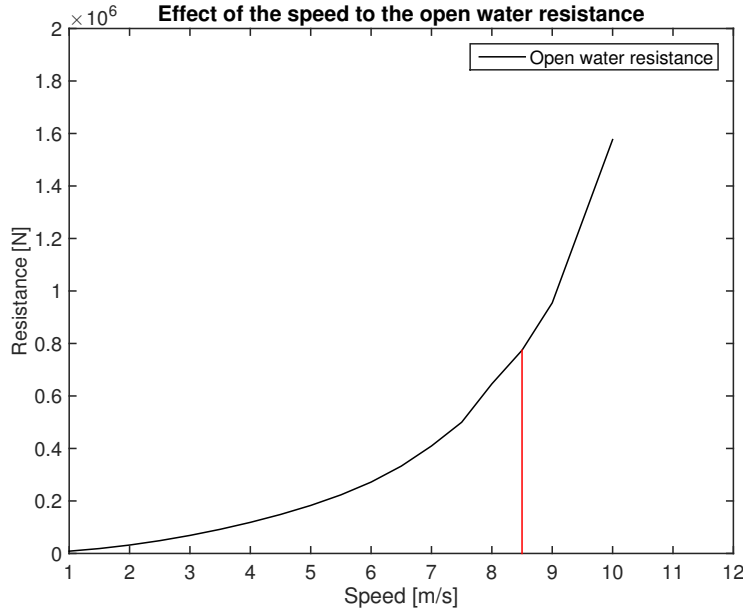


Figure 8.6: Effect of the speed to the open water resistance (red line indicates the used open water speed in this thesis, 8.5 m/s).

8.3 Models to solve fuel and economic efficiency

In this section, models used to solve fuel consumption and economical efficiency are presented.

8.3.1 Fuel consumption

DAS

To get the fuel consumption of DAS, the speed in full power and with 80 % of power in different ice conditions are calculated. With method by La Prairie et al. (1995) first the ice field is generated for each segment on each month with method described in section 8.1. For all cases this is run for 100 ridge fields with same input data to get a good number of results in different fields. The output of the simulation were average speed, standard deviation of the average and the number of cases the ship got stuck in ice. All ice conditions used in the model can be found from appendix A. For method by Kotovirta et al. (2009) first the equivalent thickness is solved and then the speed is simulated with the help of resistance equations.

To get the resistance the vessel has to overcome equation (8.16) is used. The used velocity is solved with equation of motion.

$$\mathbf{s} = \mathbf{s}_0 + \mathbf{v}_0 t + \frac{\mathbf{a}t^2}{2} \quad (8.23)$$

$$\mathbf{v} = \mathbf{a}t + \mathbf{v}_0 \quad (8.24)$$

Variables of equations (8.23) and (8.24) can be found from table 8.9.

Table 8.9: Variables of equations (8.23) and (8.24).

Variable	Description
\mathbf{a}	Acceleration vector
\mathbf{s}	Final position vector
\mathbf{s}_0	Initial position vector
\mathbf{v}	Final velocity vector
\mathbf{v}_0	Initial velocity vector
Δt	Time interval

Acceleration of the vessel can be determined from equation

$$a = F/m \quad (8.25)$$

where m is the mass of displacement of the vessel and F can be determined from

$$F = T_{net} - R_{tot} \quad (8.26)$$

T_{net} is the net thrust of the ship which has to be greater than the total resistance for the ship to be able to move in ice. The net thrust can be estimated by the following approximative formula (Kotovirta et al. 2009)

$$T_{net}(v) = \left(1 - \frac{1}{3} \frac{v}{v_{ow}} - \frac{2}{3} \left(\frac{v}{v_{ow}} \right)^2 \right) \cdot T_{pull} \quad (8.27)$$

where pollard pull, T_{pull} , of the vessel is given or calculated using the formula

$$T_{pull} = K_e (P_s D_P)^{2/3} \quad (8.28)$$

The assumption is that by first solving the diameter of the propeller, D_P , with the pollard pull in full power, from equation (8.28), new pollard pull can be calculated for 80 % power, by multiplying propulsion power, P_s , with 0.8. In equation (8.28) value 0.702 is used for the empirical quality coefficient of the pollard pull, K_e (Kujala and Riska 2010).

Ice concentration, see Chapter 4, affects to the ship velocity by the way presented by Kotovirta et al. (2009)

$$f(x) = \begin{cases} v_{ow} & : C \leq C_0 \\ \frac{(C_{00}-C)v_{ow}+(C-C_0)v_{i,eq}}{C_{00}-C_0} & : C_0 < C < C_{00} \\ v_{i,eq} & : C \geq C_{00} \end{cases}$$

where C_0 is 70 % concentration and C_{00} 95 %. C is the real concentration on the examined area. As can be seen from above if a ship operates in open water conditions or C is less than 70 %, then the power requirements are solved with equation (8.22) for speed 8.5 m/s.

If DAS got stuck in ice the assumption is that it is then escorted by an icebreaker through that sea area with speed of 4 m/s (Riska 2010a). In this thesis the assumption is that if the ship got stuck in ice on over 25 % of 100 simulations it is not able to sail independently on that area. The output, average velocity, of simulation with 100 ice fields takes only into account the values that are greater than zero. The number of zeros are also output and it is used to estimate the capability the DAS to sail independently.

Ice-bow ship

For this vessel the simulations are similar to the DAS. However, only the method presented by La Prairie et al. (1995) is used for the simulation to get the speed of this vessel. Only the one with full propulsion power is simulated. The resistance this ship needs to overcome is solved in bow-first mode and therefore equation (8.14) is used. The effect of the concentration and getting stuck are similar to the DAS.

Open water ship

This ship operates only in ice-free waters and therefore after the resistance is calculated with equation (8.22) the power requirement can be solved for open water speed, 8.5 m/s. The required power can be calculated with equation

$$P_{ow} = R_{ow} \cdot v_{ow} \tag{8.29}$$

Assisted ship

Assumption is that the vessel is escorted by an icebreaker through ice field and therefore this ship encounters only brash ice, *i.e.*, channel without consolidated layer. Resistance is solved with equation (8.17). Speed is assumed to be 4 m/s which is suggested to be a suitable speed for icebreaker assistance (Riska 2010a). Channel is formed from brash ice and it is built with the same method as ridge field presented by La Prairie et al. (1995). The assumption is that icebreaker only breaks the ice field to brash ice and the thickness is based on the ridge generator, *i.e.*, icebreaker does not affect to the thickness of the field. Between ridges the assumption is that brash ice thickness in channel is equal to the thickness of level ice on that area.

The vessel sails in ice covered waters only part of the year, see Chapter 6. In channel the output of the simulation is the power demand to overcome the resistance the channel causes with the escort speed. The total resistance consists of channel resistance, equation (8.17), and open water resistance, (8.22), with the escort speed. In open water, the power demand is solved similarly to that of open water ship. The power requirement for channel operations is solved with equation

$$P_{ch} = (R_{ch} + R_{ow \text{ escort speed}}) \cdot v_{\text{escort speed}} \quad (8.30)$$

Fuel consumption

After speed for DAS and ice-bow ship, in different sea areas for each month is solved, the time spent on each leg can be calculated with

$$t = \frac{s}{v} \quad (8.31)$$

where t is time, s is length and v is velocity.

Also for open water ship and assisted ship time spent on certain parts of the route can be solved with equation (8.31). In open water conditions v is 8.5 m/s and in channel 4 m/s. Fuel consumption can then be solved with equation

$$\dot{m}_{fuel} = SFOC \cdot t \cdot P \quad (8.32)$$

The variables of the equation (8.32) are given in table 8.10.

Table 8.10: Variables of equation (8.32).

Variable	Description
\dot{m}_{fuel}	Fuel consumption in grams
P	Propulsion power in kW, for DAS and ice-bow ship full power 13 000 kW and 10 400 kW, for the comparison with 80 % of the full power. For open water ship 5923 kW, with speed of 8.5 m/s, and for assisted ship in channel it is case dependent
$SFOC$	Specific Fuel Consumption in g/kWh, here 174 g/kWh (Wärtsilä 2015)
t	Time spent on leg in hours

8.3.2 Economical model

The operational costs include operating, voyage and cargo handling costs. Capital repayments cover interest and periodic maintenance of the ship. The cost of running a shipping company depends on a combination of three factors. First, the ship sets the broad framework of costs through its fuel consumption, the number of crew required to operate it and its physical condition, which dictates the requirement for repairs and maintenance. Second, inflation in the cost of bought-in items, particularly bunkers, consumables, crew wages, ship repair costs and the interest rates, all of which are subject to economic trends outside the control of the shipowner. Third, costs depend on how efficiently the owner manages the company, including the administrative overhead and operational efficiency. The costs can be classified into five categories (Stopford 1997):

- Operating costs, which constitute the expenses involved in the day-to-day running of the ship - essentially those costs such as crew, stores and maintenance.
- Periodic maintenance costs, which are incurred when the ship is dry-docked for major repairs, usually at the time of its special survey.
- Voyage costs are variable costs associated with a specific voyage that include such items as fuel, port charges and canal due.
- Capital costs depend on the way the ship has been financed.
- Cargo handling costs, represent the expense of loading, stowing and discharging cargo.

In this thesis the economical calculations are limited to voyage and operating costs. The total costs can be solved with equation

$$C_{USD} = FC + OC + IC + CD \quad (8.33)$$

The variables of equation (8.33) are presented in table 8.11.

Table 8.11: Variables of equation (8.33).

Variable	Description
C_{USD}	Total costs
CD	Canal dues
FC	Fuel costs (limited to the ones caused by the ship movement)
IC	Icebreaker cost
OC	Operational costs (insurance, crew, <i>etc.</i>)

In this thesis the fuel costs are limited to the ones caused by the fuel needed for the ship to overcome the resistance. For the economical examination the ship is assumed to use only HFO. The price for HFO is calculated with the current price - 350 USD per ton. For comparison the price on May 2014 was used - 600 USD per ton (Statistics and Studies 2015).

According to the Northern Sea Route Information Office (2015) the fee on the NSR consists of the need for icebreaker support. On the Suez Canal route the fee depends on the net tonnage of the vessel. This fee is solved for the case vessel with the toll calculator presented in Suez Canal Authority (2015).

Used icebreaker escort fee for one trip on the NSR is close to 500 000 USD (Way et al. 2015), which means that it is about 86 USD for one kilometre. This kilometre charge is based on the total amount of ice covered kilometres on the NSR. For operating costs such as crew salary and insurance the used values are 7140 USD per day for NSR operations and 4880 USD per day on the SCR. These costs are based on Way et al. (2015), where the used costs are 6100 USD for non-ice class vessel and 8925 USD for ice class vessel, however, these were for a bigger vessel and hence the value is multiplied with 0.8 to get the costs used in this thesis. The difference between operation costs of ice-class and non-ice class vessel, is due to the more expensive insurance *etc.* costs with an ice-class ship.

In table 8.12 the prices used in this thesis are presented

Table 8.12: Prices for shipping.

Price	
Fuel price per ton	350 and 600 USD/ton
Icebreaker cost	86 USD/km
Operating costs on the NSR	7140 USD/day
Operating costs on the SCR	4880 USD/day
SCR fees	94 000 USD/trip

Chapter 9

Results

In this chapter, simulation results for fuel and economic efficiency are presented. First, individual results for each ship is introduced. After those the results are gathered together and compared.

9.1 DAS

For DAS, the speed on each segment in ice was first solved, as explained earlier in Chapter 8. Assumption was that the ship uses full power in ice, *i.e.*, propulsion power 13 000 kW. For comparison speed and fuel consumption with 80 % of propulsion power were solved for average winter. This was done to see the capability of the DAS to sail in ice with lower propulsion power. While sailing in open water conditions the power demand was solved with equation (8.29). Speeds with full power were simulated using two different ridge field generating methods, the one presented by La Prairie et al. (1995) and Kotovirta et al. (2009). The difference of the output from these two methods can be seen in figure 9.1, table 9.1 and figure 9.2. Input parameters for figure 9.1 for both cases are the same and can be found from table 8.4.

As can be seen from figure 9.1 the speeds simulated with the method by La Prairie et al. (1995) varies much according to the generated ridge field. Because of the variation, the simulation was run with 100 different ridge fields and output was the average from all of the cases, except the ones where the speed was zero. Also the standard deviation of the speed was one output. Fuel consumption was calculated also with the values given by average \pm standard deviation. However, these results were so close to the ones with average speed that it did not effect the fuel consumption. In table 9.1 averages of the velocities of methods by La Prairie et al. (1995) and Kotovirta et al. (2009) can be seen. The averages were calculated only for cases where both simulations gave a value where the ship did not get stuck in ice. The open water areas were neglected from averages because they were the same in both cases. The percentage of cases where the ship got stuck is also presented.

Using the method of La Prairie et al. (1995) the assumption was that if the vessel got stuck in ice, on some segment over 25 % of the simulated 100 cases, it can not operate independently on that sea area. Then it is escorted through it by an icebreaker with speed of 4 m/s.

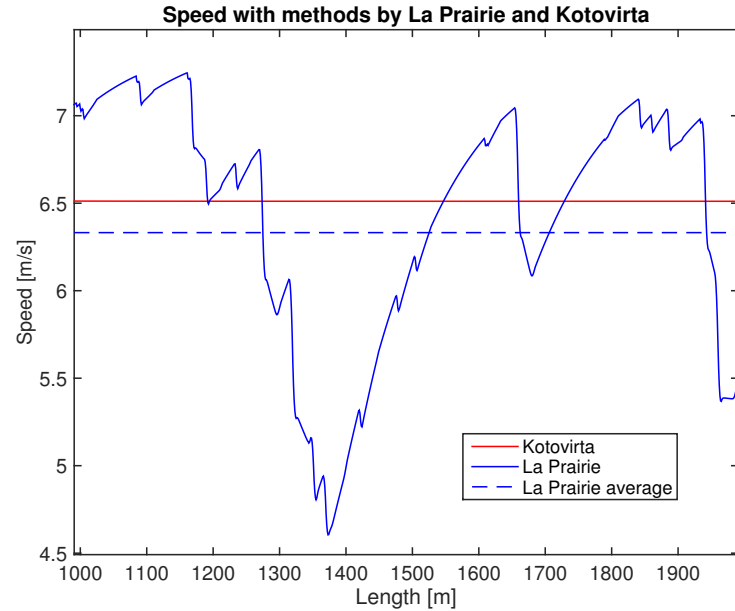


Figure 9.1: Speeds for one segment solved for ice fields generated with methods by La Prairie et al. (1995) and Kotovirta et al. (2009).

Table 9.1: Comparison of the two used methods. For each sea area the results are for whole year. LP states for the method presented by La Prairie et al. (1995) and K for Kotovirta et al. (2009).

Sea area		$v_{AVE,LP}$ [m/s]	Stuck %	$v_{AVE,K}$ [m/s]	Stuck %
Bering St	average	7.9	0	8.0	0
	severe	7.2	56	7.6	0
Chukchi	average	0	100	6.9	50
	severe	0	100	5.3	64
East Siberia	average	7.5	78	7.7	56
	severe	0	100	5.2	64
Laptev	average	6.9	0	6.6	0
	severe	0	100	5.8	45
Kara East	average	0	100	6.6	50
	severe	0	100	5.4	73
Kara Centre	average	7.1	0	7.1	0
	severe	6.8	45	6.7	0
Kara West	average	7.6	0	7.6	0
	severe	6.3	0	6.0	0
Kara Gate	average	0	100	6.8	0
	severe	0	100	7.0	60
Pechora	average	8.0	0	8.0	0
	severe	7.7	0	7.7	0

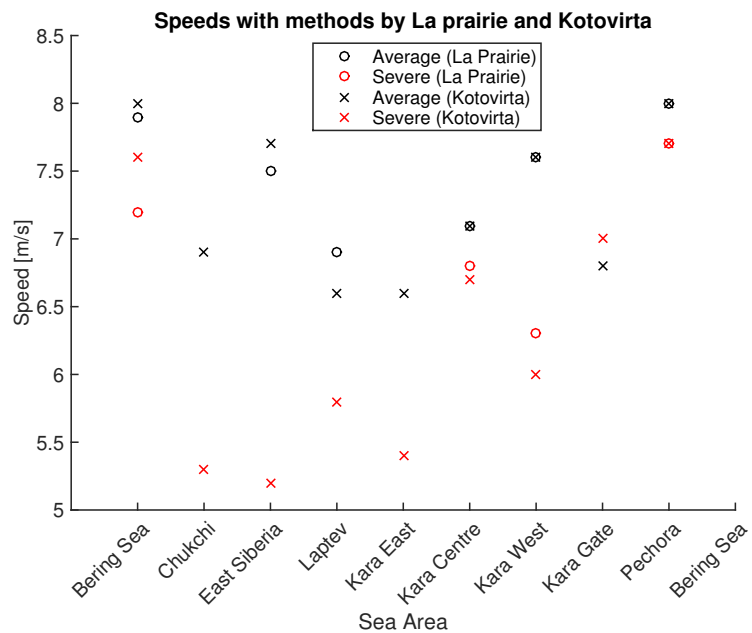


Figure 9.2: Speeds solved for ice fields generated with methods by La Prairie et al. (1995) and Kotovirta et al. (2009). The missing speed means that the vessel is stuck in ice.

In tables 9.2, 9.3, 9.4, 9.5 and 9.6 days and fuel consumption caused by ship movement for one trip, fuel consumption per day and icebreaker escorted kilometres and their percentage of total kilometres of one trip, *i.e.*, 13 149 km, can be seen. Table 9.2 contain simulation results for DAS with full power on average winter where the ridge field is generated with method presented by La Prairie et al. (1995). Table 9.4 shows the same for severe winter. Results for average winter with 80 % of power is presented in table 9.3, this was also simulated with ridge field generated by method of La Prairie et al. (1995). For DAS the results for average and severe winter simulated with ridge field generated with method by Kotovirta et al. (2009) are presented in tables 9.5 and 9.6.

Table 9.2: Results with full power for average winter (La Prairie).

Month	Days	\dot{m}_{fuel} [tons]	tons/day	IB escort [km] (%)
Jan	22	684	31	2372 (18)
Feb	22	741	33	2372 (23)
Mar	22	794	35	2372 (23)
Apr	23	817	36	2372 (23)
May	23	817	36	2372 (23)
Jun	23	810	36	2372 (23)
Jul	20	540	27	1152 (9)
Aug	18	443	25	-
Sep	18	443	25	-
Oct	18	443	25	-
Nov	20	605	30	1127 (9)
Dec	20	683	33	1220 (9)

Table 9.3: Results with 80 % of power for average winter (La Prairie).

Month	Days	\dot{m}_{fuel} [tons]	tons/day	IB escort [km] (%)
Jan	22	631	29	2372 (18)
Feb	22	688	31	2372 (18)
Mar	23	740	33	2372 (18)
Apr	23	764	33	2372 (18)
May	23	763	33	2372 (18)
Jun	23	757	33	2372 (18)
Jul	20	530	27	1152 (9)
Aug	18	443	25	-
Sep	18	443	25	-
Oct	18	443	25	-
Nov	20	553	28	1127 (9)
Dec	22	593	27	2372 (18)

Table 9.4: Results with full power for severe winter (La Prairie).

Month	Days	\dot{m}_{fuel} [tons]	tons/day	IB escort [km] (%)
Jan	24	774	32	3441 (26)
Feb	25	804	32	4628 (35)
Mar	26	842	33	4628 (35)
Apr	26	864	34	4628 (35)
May	26	857	34	4628 (35)
Jun	25	848	33	4628 (35)
Jul	24	811	34	3441 (26)
Aug	23	683	30	3348 (25)
Sep	18	443	25	-
Oct	23	601	26	3441 (26)
Nov	24	696	29	3441 (26)
Dec	24	721	30	3441 (26)

Table 9.5: Results with full power for average winter (Kotovirta).

Month	Days	\dot{m}_{fuel} [tons]	tons/day	IB escort [km] (%)
Jan	20	784	39	-
Feb	22	804	37	1152 (9)
Mar	22	798	36	2279 (17)
Apr	23	830	36	2279 (17)
May	23	829	36	2279 (17)
Jun	23	822	36	2279 (17)
Jul	18	539	29	-
Aug	18	443	25	-
Sep	18	443	25	-
Oct	18	443	25	-
Nov	18	636	35	-
Dec	19	716	38	-

Table 9.6: Results with full power for severe winter (Kotovirta).

Month	Days	\dot{m}_{fuel} [tons]	tons/day	IB escort [km] (%)
Jan	24	841	35	2279 (17)
Feb	25	869	35	3441 (26)
Mar	25	917	36	3441 (26)
Apr	26	956	37	3441 (26)
May	26	952	37	3441 (26)
Jun	25	920	37	3441 (26)
Jul	23	866	37	2372 (18)
Aug	20	722	36	-
Sep	18	443	25	-
Oct	19	662	36	-
Nov	22	883	41	-
Dec	24	953	40	442 (3)

9.2 Ice-bow ship

First the speed, the ship uses on each segment is solved. Only the full propulsion power was studied. In open water conditions equation (8.29) was used to get the power demand. For this vessel the ridge field was only generated with method by La Prairie et al. (1995) for the simulations. Assumption was that if the vessel got stuck on over 25 % of the simulated 100 runs it can not sail independently and then the icebreaker assistance is needed. The power demand on escort situation was solved with equation (8.30). In tables 9.7 and 9.8 the results for the fuel consumption for average and severe winter, days to make one trip, consumed fuel per one day and icebreaker escorted kilometres and their percentage of the total length of the NSR are presented.

Table 9.7: Results for vessel with an ice-bow on average winter.

Month	Days	\dot{m}_{fuel} [tons]	tons/day	IB escort [km] (%)
Jan	22	729	33	3199 (24)
Feb	22	793	36	2862 (22)
Mar	22	850	38	3141 (24)
Apr	23	880	39	3010 (23)
May	23	880	39	3105 (24)
Jun	22	864	38	3029 (23)
Jul	20	579	29	1728 (13)
Aug	18	492	27	-
Sep	18	492	27	-
Oct	18	492	27	-
Nov	22	611	28	3037 (23)
Dec	20	717	35	1765 (13)

Table 9.8: Results for vessel with an ice-bow on severe winter.

Month	Days	\dot{m}_{fuel} [tons]	tons/day	IB escort [km] (%)
Jan	24	828	34	4247 (32)
Feb	26	882	34	5385 (41)
Mar	26	916	35	5956 (45)
Apr	26	946	36	5765 (44)
May	26	944	37	5406 (41)
Jun	25	939	37	5247 (40)
Jul	25	885	36	4969 (38)
Aug	23	790	34	4314 (33)
Sep	18	492	27	-
Oct	23	662	28	4401 (33)
Nov	24	753	32	4183 (32)
Dec	24	774	32	4281 (33)

9.3 Open water ship

For open water ship first the power demand was solved. Assumption was that the conditions on the SCR are constant and therefore the needed power is simulated with the resistance the water causes to the hull with constant open water velocity, in here 8.5 m/s. In table 9.9 the power demand, days for one voyage, fuel consumption caused by the the vessel overcoming the resistance on one voyage and fuel consumption per day are shown. Assumption is that all the values presented in table 9.9 are the same on every month.

Table 9.9: Power demand, time and fuel consumption for one voayge and fuel consumption per day.

Power demand [kW]	Days	\dot{m}_{fuel} [tons]	tons/day
5923	29	711	25

9.4 Assisted ship

Assumption was that this ship is escorted by an icebreaker through ice. The ship uses the SCR from January until end of June and on December. From July until late November it uses the NSR. Escort speed was assumed to be 4 m/s (Riska 2010a). For this vessel the power requirement was solved for open water and for channel conditions. In tables 9.10 and 9.11 results for fuel consumption caused by the movement of the ship, the time spent on one voyage and fuel consumption per day are shown on average winter and for severe winter. Note that the ridge field for this ship was generated with the method of La Prairie et al. (1995).

Table 9.10: Results of the simulations for average winter.

Month	Route	Days	\dot{m}_{fuel} [tons]	tons/day
Dec-Jun	SCR	29	790	27
Jul	NSR	20	578	29
Aug	NSR	18	492	27
Sep	NSR	18	492	27
Oct	NSR	18	492	27
Nov	NSR	25	540	22

Table 9.11: Results of the simulations for severe winter.

Month	Route	Days	\dot{m}_{fuel} [tons]	tons/day
Dec-Jun	SCR	29	790	27
Jul	NSR	27	877	33
Aug	NSR	24	774	32
Sep	NSR	18	492	27
Oct	NSR	25	625	25
Nov	NSR	27	650	24

9.5 Comparing results

In this section, the results presented above are compared. The comparison is done by plotting the results from different cases to same figures. In figure 9.3 is plotted results of fuel consumption per day on average winter. Plotted results include the ones for DAS with full power with both studied methods, the one for 80 % of propulsion power with method by La Prairie et al. (1995) and the ones for ice-bow ship, open water ship and assisted ship. Red color indicates that DAS or ice-bow ship needs icebreaker assistance at some point on the voyage. The need for the icebreaker assistance can occur on one or multiple segments. The icebreaker escorted kilometres can be seen from table 9.12.

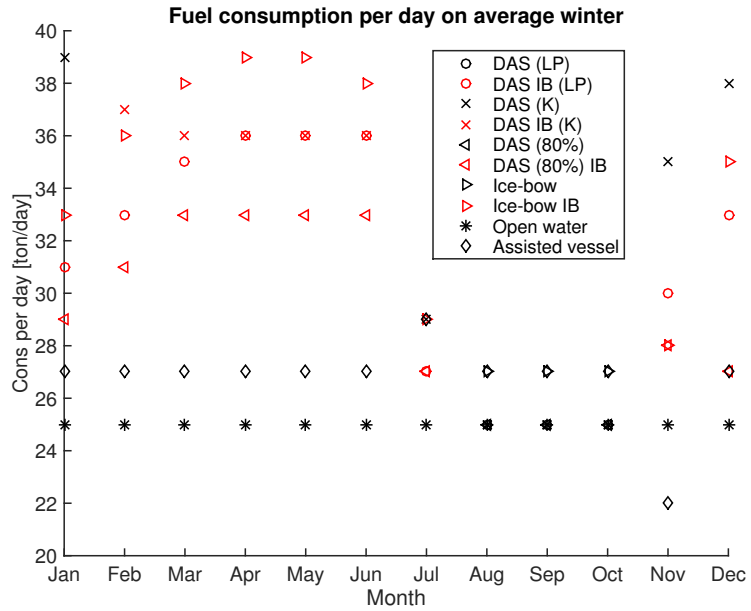


Figure 9.3: Consumption per day for average winter for all cases.

In figure 9.4 the results for consumption per day on severe winter are plotted. These results include the ones for DAS with full power simulated with both methods and also the ones for ice-bow, open water and assisted ships. Note that the winter conditions do not affect the open water ship because it only sails on the SCR. Red color indicates that DAS or ice-bow ship needs icebreaker help during some part of the voyage.

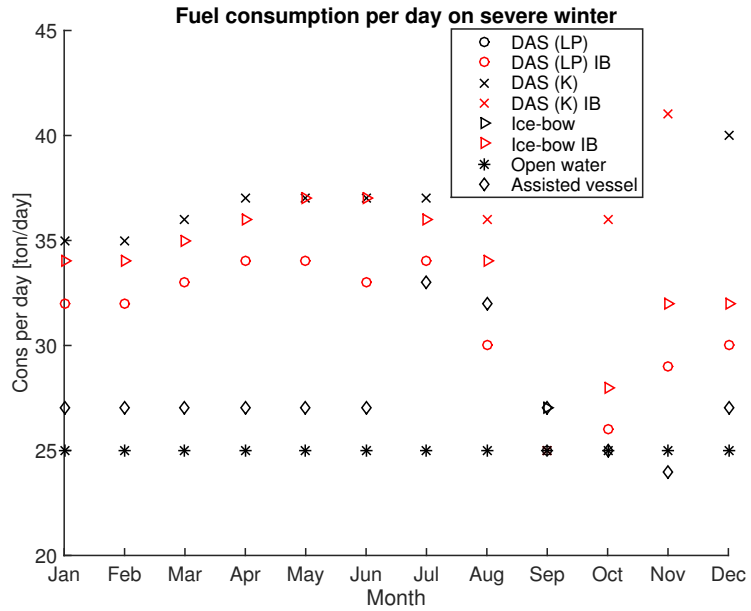


Figure 9.4: Consumption per day for severe winter for all cases.

In table 9.12 the results for number of trips made by each studied vessel on chosen route per year can be seen. It also contains results for the number of TEUs possible to deliver during one year, these are calculated with the assumption that all the vessels carry 750 TEUs for every trip, *i.e.*, from Europe to Asia and vice versa. The assumption is that the vessels spends only one day at the harbor. Table 9.12 consist also results of the fuel consumption per year and fuel consumption per one TEU per year.

Table 9.12: Results for one year operations.

	Trips	TEUs	\dot{m}_{ton}	\dot{m}_{ton}/TEU	IB need [km]
DAS average (LP)	17.0	12 732	10 824	0.85	23 437
DAS average 80 % power (LP)	16.8	12 616	10 092	0.80	24 379
DAS average (K)	17.5	13 128	11 541	0.88	13 192
AS average	14.6	10 950	9 475	0.87	6 321
Ice-bow average	16.9	12 660	11 553	0.91	24 876
OW	12.2	9 125	8 727	0.96	-
DAS severe (LP)	14.8	11 062	10 832	0.98	51 880
DAS severe (K)	15.4	11 579	12 593	1.09	26 026
AS severe	13.3	9 968	9 688	0.97	23 064
Ice-bow severe	14.7	10 995	11 806	1.07	54 154

For the economic calculations prices from table 8.12 were used. The calculations were done for whole year. Also the voyage costs for one TEU were solved. The number of TEUs delivered for each case can be seen in table 9.12. As for HFO price two different values were used, the current (referred as F1) and the one from May 2014 (F2). For each studied case, the price was a sum of price of the consumed fuel, operating costs, icebreaker support if needed and the canal fee on the SCR, see equation (8.33). According to Northern Sea Route Information Office (2015) the fee to use the NSR consists only of icebreaker support. In this thesis assumption was that the icebreaker cost consists only of the escorted kilometres.

In table 9.13 the voyage costs for each case for both winters are gathered. Included costs in the table are total costs for one year and per TEU for both fuel prices. In figures 9.5 and 9.6 the costs are presented per one TEU with two fuel prices for both winters.

Table 9.13: Results for economic calculations.

	$\text{Tot}_{F1}[\text{USD}]$	$\text{Tot}_{F2} [\text{USD}]$	USD/TEU_{F1}	USD/TEU_{F2}
DAS average (LP)	8 400 062	11 106 062	660	872
DAS average 80 % power (LP)	8 224 471	10 747 471	652	852
DAS average (K)	7 774 322	10 659 572	592	812
AS average	6 648 714	9 017 464	607	824
Ice-bow average	8 778 352	11 666 601	693	922
OW	5 982 450	8 164 200	656	895
DAS severe (LP)	10 836 800	13 544 800	980	1 224
DAS severe (K)	9 240 759	12 389 009	798	1 070
AS severe	8 156 944	10 578 944	818	1 061
Ice-bow severe	11 372 292	14 323 792	1 034	1 303

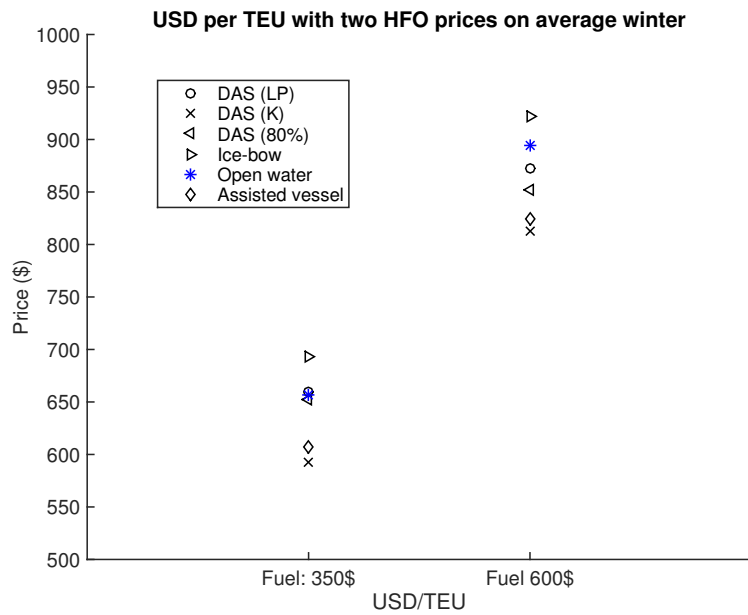


Figure 9.5: Cost for shipping per one TEU for different cases for average winter.

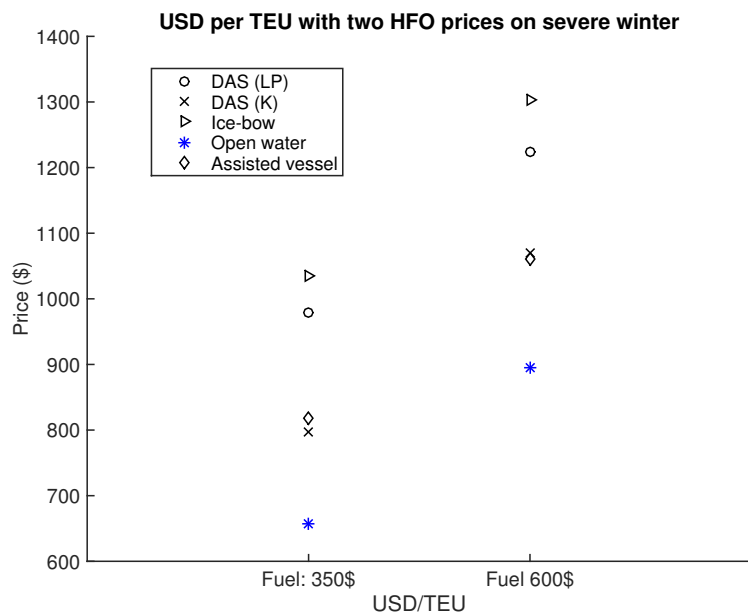


Figure 9.6: Cost for shipping per one TEU for different cases for severe winter.

Chapter 10

Analyses of the results

In this chapter, the results presented in Chapter 9 are analysed. First, the comparison of the two used methods to generate the ridge field for simulations is done. This is followed by a discussion of the results for the fuel efficiency. After that analysing of the economical efficiency is done. Finally, the fuel and economical efficiencies are compared together.

The efficiencies were investigated for four different cases:

- A double acting ship operating year-around on the Northern Sea Route.
- An ice-bow ship operating year-around on the Northern Sea Route.
- An open water ship operating year-around on the Suez Canal route.
- A ship with an ice-bow operating from July until late November on the NSR escorted by an icebreaker through ice. During the rest of the year, the vessel uses the Suez Canal route. This part of the year operation is due the current regulations on the NSR.

10.1 La Prairie vs Kotovirta

For DAS the simulation was done with modelling the ridge field with two different methods: the one presented by La Prairie et al. (1995) and the one by Kotovirta et al. (2009). One aim of the thesis was to compare the effect of the different methods to the simulation results. Both of these methods take into account the ridges and the level ice. For the level ice resistance calculations, the method of Lindqvist, given in equation (8.6), was used. For the ridge resistance, the method of Malmberg, given in equation (8.11), was used. Both of the simulations were done with the stern-first mode, see Chapter 8.

Method by Kotovirta et al. (2009) is much simpler to simulate and therefore time can be saved by using this one. The difference of the simulation results are presented in figure

[9.1](#) and in table [9.1](#). Speeds from the table are plotted into figure [9.2](#). From figure [9.1](#) can be seen the difference of speed in one case for both methods. Using the method by La Prairie et al. (1995) the speed varies much due to the different sizes of the ridges on the route. The speed is constant with the method by Kotovirta et al. (2009) on one segment, due to the constant thickness of the ice field. Output of the method by La Prairie et al. (1995) was the average speed of the segment and in figure [9.1](#) this is expressed with blue dashed line. Standard deviation (SD) was one output of the method by La Prairie et al. (1995). However, it was found to be close enough to the results that it did not affect the fuel consumption significantly. All results, with average and average plus-minus SD speeds in one segment, for fuel consumption was within one ton. From the results can be seen that the average speed simulated with both methods corresponds quite well with each other.

With the method presented by Kotovirta et al. (2009) DAS can operate independently in all areas at least on some month during the year, but with method by La Prairie et al. (1995) it needs icebreaker escort on average winter in four areas year-around and on severe winter in five areas. One notable difference is the Kara Gate on average winter, when DAS cannot operate at all independently with the method by La Prairie et al. (1995) and is able to operate independently all the time with the method by Kotovirta et al. (2009). In that area the level ice thickness is below 1.0 metre but the thickness of the ridges are quite high during all ice months, see figure [4.6](#) and appendix [A](#). Also the ridge density is high on Kara Gate, see figure [4.7](#), and as can be seen from equation [\(8.5\)](#) the ridge density does not have as big effect to the equivalent thickness as the mean ridge thickness has. Also the difference how these two methods deal with the consolidated layer might be one answer to this significant difference in the results. Kotovirta et al. (2009) only flattens the ridges underneath the level ice and the consolidated layer is not taken into account at all, and in this thesis it is assumed to be 1.5 times the surrounding level ice with the method by La Prairie et al. (1995).

The method of La Prairie et al. (1995) generates the ridge field more realistically. With this method the ridge field can contain quite many and thick ridges. Ridge density and thickness are also input for the method by Kotovirta et al. (2009), but the ship is more able to operate when the thickness is constant (Lensu 2003).

The conclusion of the comparison of the two ridge generating methods is that with very light ice conditions these could be used equally. With average and more severe ice conditions La Prairie et al. (1995) is more conservative. Due to this for the fuel and economic analyses only the DAS simulated with the method by La Prairie et al. (1995) is taken into account. The difference should be investigated closer in the future and validated with model tests.

10.2 Fuel efficiency

In tables 9.2 and 9.3 fuel consumptions for DAS with full power during average and severe winters are presented. Fuel consumption for DAS with 80 % propulsion power during average winter is presented in table 9.4. The fuel efficiency for open water ship sailing along the SCR is presented in table 9.9 and the results for assisted ship for both winters in tables 9.10 and 9.11. The comparison of fuel consumed per day for all cases is plotted in figure 9.3 for average winter and for severe in figure 9.4.

From the results can be seen that the consumption per day on both average and severe winter is smallest for the open water ship sailing via the SCR. However, on November the assisted ship has smallest consumption per day. This is due the light ice conditions on November and in ice it is assisted with speed of 4 m/s. Slow steaming decreases the resistance and hence saves fuel. Effect of the speed to the open water resistance can be seen from figure 8.6. Slow steaming affects also in ice by decreasing the power demand and hence saves the fuel.

Assisted ship uses the SCR from December until July, *i.e.*, same as the open water ship. Both of these vessels sail the same speed in open water and hence the time for the trip is equal. However, as noted in Chapter 6, the assisted ship does not have a bulbous bow. In this thesis, the assumption was that the open water resistance without a bulb is higher compared to the bulbous bow. Lack of the bulb increases the consumption per day with 2 tons on one trip on the SCR.

The biggest fuel per day consumption is in most cases with the ice-bow ship. From the results can be seen that DAS is much more fuel efficient than the ice-bow ship. The biggest need for icebreaker escort is with the ice-bow ship. This is during both winters. A notable result is that ice-bow ship needs icebreaker more than DAS with decreased propulsion power.

From figure 9.3 can be seen that the consumption per day is in every month less or the same with 80 % of propulsion power compared to the full propulsion power. The icebreaker need is only approximately 4 % higher with decreased propulsion power.

A value that is in great interest is how many tons of fuel is used for one TEU per year. This was solved with help of the trips the vessel is able to make during one year. Assumption was that the harbor time is one day for each case and no maintenance times, icebreaker or canal waiting times *etc.* are taken into account. With the number of trips the total amount of TEUs delivered can be solved. After the total fuel consumption per year is known, the amount of consumed fuel in tons, \dot{m}_{ton} , per one TEU can be calculated with help of delivered TEUs. These results are presented in table 9.12.

From table 9.12 can be seen that the most fuel efficient way to import one TEU during average winter is with DAS using 80 % of propulsion power. The next best is DAS with full power. DAS with full power consumes about 10 % less fuel per TEU compared to the ice-bow ship. During average winter open water ship sailing via the SCR is the poorest and it consumes fuel per TEU almost 20 % more than DAS with 80 % of the propulsion power.

On severe winter DAS with full power is the best alternative. Open water and assisted ship are within 1 %, what comes to the fuel consumption per one TEU on severe winter. Year-around navigation along the NSR with DAS consumes almost 10 % less fuel per TEU than with an ice-bow ship.

10.3 Economical efficiency

The economical investigation was done by calculating how much it costs to deliver one TEU from Europe to Asia. As mentioned in Chapter 8, costs were limited only to the voyage and operating costs, *i.e.*, fuel price caused by the ship overcoming the resistance, insurance and crew costs, cost of icebreaker assistance (only on the NSR) and canal fee (only on the SCR). The calculations were done using the current HFO price and for comparison the one from May 2014. In table 9.13 can be seen the results of the economical calculations. In figures 9.5 and 9.6 the costs to ship one TEU with both fuel prices on both winters are plotted.

From the results can be seen that economically the best one is assisted ship using both routes during the year. Results shows that DAS with decreased power is more economically efficient during the average winter than with the full propulsion power. During average winter the ice-bow ship is the least economically efficient. The difference between the DAS and the ice-bow ship is approximately 5 %. With more expensive fuel, assisted ship is still the most efficient from economical point of view and ice-bow ship the least efficient. However, using the NSR year-around with DAS becomes more profitable with higher fuel price compared to using only the SCR, due the good fuel efficiency.

On the severe winter the open water ship using the SCR is superior compared to other cases what comes to the costs for shipping one TEU per year. This is due the very harsh ice conditions lasting the whole year. There are only some sea areas free of ice during the year on the NSR, and therefore ships sailing there need lots of icebreaker assistance and consume lots of fuel, see table 9.12. The next best is the assisted ship which is about 10 % less economical efficient. The ice-bow ship is the poorest during the severe winter. Using the SCR year-around is almost 30 % more economically efficient than using the NSR

year-around with DAS. With more expensive fuel the results are quite similar for severe winter, due to the bigger dispersion in the economic efficiency than on average winter.

The difference with results for two different fuel prices is significant, as can be seen from figures 9.5 and 9.6. Overwhelmingly the biggest part of operation and voyage costs are due to fuel price and consumption. The fuel price varies much as can be seen from the current price and the one on May 2014.

10.4 Summary

The conditions on the NSR have a big effect on both the fuel and the economical efficiency. Even during severe winter the DAS consumes less fuel per TEU compared to the open water ship sailing on the SCR year-around. This is due to icebreaker assistance, when the ship follows an icebreaker with 4 m/s speed on brash ice. The ice-bow ship would not be a suitable alternative for shipping via Europe and Asia regardless is it an average or severe winter.

During the average winter DAS becomes more preferable alternative, and with 80 % of propulsion power the fuel consumption per one TEU is superior compared the other cases. However, assisted ship is the best from an economical point of view, despite the lower efficiency in open water. This is due its good performance in every aspect; it can do quite many trips per year, it uses almost 40 % shorter NSR only during months with quite light ice conditions, *i.e.*, no need for icebreaker support on the whole trip via the NSR, and it is quite fuel efficient. In the future the rules dealing with emissions will tighten, see Chapter 2, and then a more fuel efficient way for shipping would become also more economically efficient. The results indicate that if the fuel price increases the DAS becomes more and more reasonable alternative for shipping.

The assisted ship was expected to follow the icebreaker bow first. However, as the results show the stern-first operation is more efficient in ice. An assumption can be made that DAS could be a suitable concept for sailing part of the year via the NSR and rest using the SCR. DAS would move stern first while escorted by an icebreaker.

Chapter 11

Conclusions

The aim of this thesis was to find the most fuel efficient way for shipping from Europe to Asia. After that the economical efficiency was solved. For the analyses four different cases were studied: A double acting ship operating year-around on the NSR, a vessel with an ice-bow operating year-around on the NSR, an open water ship using the SCR and an assisted ship using part of the year the NSR and rest the SCR. Above mentioned cases were chosen to compare the effectiveness of the DAS-concept in ice to a typical ice-bow vessel. Open water ship using the SCR was taken into account to compare two different routes connecting Europe to Asia: the NSR and the SCR. Due to the rules of the navigation on the NSR, currently a vessel could not be sailing independently year-around there and therefore an assisted ship was also taken into account to the study.

Simulating performance of the ship in ice is challenging, and there are multiple ways to approach this subject. One aim of this thesis was to compare the feasibility of two different ice field generation methods presented by La Prairie et al. (1995) and Kotovirta et al. (2009). These two methods approach the generation procedure from different angles: La Prairie et al. (1995) generates the ice field to be as realistic as possible, consisting both level ice and random number of different size ridges, while Kotovirta et al. (2009) flattens the ridge field, so that the ice field consists of level ice and ridged ice with constant thickness. This comparison was done because to the knowledge of the author there are no publications where this has been studied earlier. In addition, by using the method by Kotovirta et al. (2009), time can be saved with the simulation procedure. For both ice fields the method by Lindqvist (1989) was used to solve the level ice resistance. For ridge resistance method by Malmberg (1983) was used. The resistance equations were used in astern-mode with alterations of the method by Tan et al. (2014).

There are only limited number of publications dealing the double acting ship. None of these publications that the author is aware of examines the performance of such vessel in the ridge field. For the level ice resistance on astern mode method from Tan et al. (2014)

was used. However, this is based only on one series of model tests. For ridge resistance in astern mode the author found out a coefficient based on the effect of the stern-first movement to the level ice resistance. The assumption was that the stern-first operation affects only the part that encounters the ridge first, in this case stern, and the coefficient was used in the ridge resistance equation impacting on this area. The same coefficient was used to find the effect of the astern mode to the channel resistance. This coefficient should be validated with model tests.

The sea and weather conditions on the SCR were not taken into account in this thesis and therefore the results for the vessels using that route might be a bit optimistic. Also the waiting times on the Suez Canal and waiting of an icebreaker, when needed, were not taken into account. Hence, the number of trips a ship can perform during one year are the maximum ones. No maintenance costs were taken into account from the economical point of view and these might be higher for vessels operating in ice compared to the ones sailing only in open water conditions. Also the building costs *etc.* would be higher for ice strengthened ships.

For fuel consumption only the consumed fuel caused by the ship overcoming the resistance was taken into account in this thesis, *i.e.*, no consumption caused by air conditioning, lighting *etc.* were accounted for. In this thesis the used fuel was only HFO, and the change of the used fuel the vessel has to do while sailing in ECA areas, explained in Chapter 2, was not taken into account. This was due to the fact that all the used ships sail approximately the same time in these areas. However, from figure 2.1 can be seen that one possible new area is the Mediterranea which is on the SCR. This might increase the costs of using this route.

An assumption was that DAS and ice-bow ship sails independently on the NSR year-around. However, the results show that they cannot, *i.e.*, in some areas during the year they need assistance from an icebreaker. However, as explained in Chapter 5, a DAS could penetrate through ridges with lower speed and the flushing and crushing effect the propellers make might help the penetration. This was taken into account in the simulations only slightly due to the lack of publications of the subject. The results for the ice-bow ship shows that it is not a suitable alternative for using the NSR year-around.

As can be seen from the results the most fuel efficient alternative is not economically the best one, because of the other related costs for shipping. However, the fuel costs covers the majority of the voyage costs and hence if the fuel price increases the most fuel efficient alternative becomes more economical efficient compared to others. During severe winter a ship using the Suez Canal route is still the best alternative, as noted also in earlier studies. However, the results show that DAS can sail independently on the NSR most of the year

when the conditions are average or lighter. From the results can even be seen that it can manage on the NSR with decreased propulsion power during average conditions. However, the studied case vessel is quite small and that affects the economical feasibility of use of the SCR. As can be seen from table 7.1 on the SCR a bigger vessel can be used compared to the NSR.

No one knows how the rules on navigations on the NSR will change in the future. The ice concentration is decreasing in the Arctic Sea. It can make the NSR ice free for several months but it might also mean increased currents and therefore more deformed ice on the route which could mean harsher ice conditions. However, the NSR is already a potential and more fuel efficient alternative compared to the SCR during average winter. If the rules change and year-around navigation would be possible, a double acting ship would be a justifiable alternative for a shipping company to use in the NSR.

Bibliography

- Arpiainen, M. and Kiili, R. (2006). *Arctic Shuttle Container Link from Alaska US to Europe*. Tech. rep. Project no. Report AARC K-63.
- Balmasov, S. (2013). "Russian NSR Transit Rules & Regulations". In: *Centre of CHNL's Arctic Logistics Information Office*.
- Briney, A. (2015). *Suez Canal Connects the Red Sea with the Mediterranean Sea*. URL: <http://geography.about.com/od/specificplacesofinterest/a/suezcanal.htm>.
- Choi, M., Chung, H., Yamaguchi, H., and Nagakawa, K. (2015). "Arctic Sea Route Path Planning Based on an Uncertain Ice Prediction Model". In: *Cold Regions Science and Technology*.
- Erikstad, S. O. and Ehlers, S. (2012). *Decision Support Framework for Exploiting Northern Sea Route Transport Opportunitie*. Tech. rep. Ship Technology Research.
- Ettema, R. and Huang, H.-P. (1990). *Ice Formation in Frequently Transited Navigation Channels*. Tech. rep. U.S. Army Corps of Engineers. Cold Regions Research & Engineering Laboratory.
- Guinness, R. E., Saarimäki, J., Ruotsalainen, L., Kuusniemi, H., Goerlandt, F., Montewka, J., Berglund, R., and Kotovirta, V. (2014). "A Method for Ice-Aware Maritime Route Optimization". In: *Position, Location and Navigation Symposium-PLANS*.
- Hasan, S. (2011). "Impact of EEDI on Ship Design and Hydrodynamics". MA thesis. Chalmers University of Technology, Gothenburg, Sweden.
- Heinänen, P. (2013). "Risteilyaluksen energiatehokkuusindeksin määrittäminen". MA thesis. Aalto-yliopisto, Insinöörityieteiden korkeakoulu.
- Hippinen, I. and Suomi, U. (2012). *Yksittäisen kohteen CO₂-päästöjen laskentaohjeistus sekä käytettävät CO₂-päästökertoimet*. Tech. rep. Motiva Oy.
- Holtrop, J. (1984). "A Statistical Re-Analysis of Resistance and Propulsion Data". In: *International Shipbuilding Progress Vol. 28*.

- Holtrop, J and Mennen, G. (1982). "An Approximate Power Prediction Method". In: *International Shipbuilding Progress*, Vol. 29, No. 335.
- Häkkinen, P. (1993). *Laivan koneistot*. Tech. rep. Raportti M-179, Otaniemi.
- Hänninen, S., Heideman, T., and Vänskä, K. (2012). "Azimuth Propeller Operation in Ice Conditions". In: *No. ICETECH12-104-RF*.
- Høyland, K. V. (2002). "Consolidation of First-Year Sea Ice Ridges". In: *Journal of Geophysical Research*, Vol. 107, No. C6, 3062, 10.1029/2000JC000526.
- IMO, a (2012a). "2012 Guidelines For The Development of A Ship Energy Efficiency Management Plan (SEEMP)". In: *Annex 9, Resolution MEPC.213(63)*.
- IMO, b (2012b). "2012 Guidelines on the Method of Calculation of the Attained Energy Efficiency Design Index (EEDI) for New Ships". In: *Annex 8, Resolution MEPC.212(63)*.
- IMO, c (2015). *IMO*. URL: <http://www.imo.org/About/Pages/Default.aspx>.
- JOULES (2015). *JOULES*. URL: <http://www.joules-project.eu/Joules/index.xhtml>.
- Juurmaa, K., Mattson, T., and Wilkman, G. (2001). "The Development of the New Double Acting Ships for Ice Operation". In: *Proceedings, The 16th International Conference on Port and Ocean Engineering Under Arctic Conditions (POAC01), August 12-17, Ottawa, Ontario, Canada*.
- Kaups, K. (2011). "Modeling of the Ship Resistance in Compressive Ice". MA thesis. Aalto University, School of Engineering.
- Kotovirta, V., Jalonen, R., Axell, L., Riska, K., and Berglund, R. (2009). "A System for Route Optimization In Ice-Covered Waters". In: *Cold Regions Science and Technology*.
- Kujala, P. and Riska, K. (2010). *Talvimerenrekku*.
- La Prairie, D., Williamson, M., Riska, K., and Petten, J. (1995). *A Transit Simulation Model for Ships in Baltic Ice Conditions*. Tech. rep. Helsinki University of Technology. Faculty of Mechanical Engineering. Ship Laboratory.
- Leiviskä, T. (2004). *Laivan propulsiorekertoimet jäissä ja avovedessä*. Tech. rep. Raportti M-287. Espoo, Finland: Teknillinen korkeakoulu, Laivalaboratorio.
- Lensu, M. (2003). "Ridge Clusters and Ice Navigation". In: *Port and Ocean Engineering under Arctic Conditions (POAC '03), Trondheim, Norway, June 16-19*.
- Lensu, M., Heale, S., Riska, K., and Kujala, P. (1996). "Ice Environment and Ship Hull Loading along the NSR". In: *Insrop Working Paper NO. 66 - 1996, 1.1.10*.

- Lindqvist, G. (1989). "A Straightforward Method for Calculation of Ice Resistance of Ship". In: *Proceedings, The 10th International Conference on Port and Ocean Engineering Under Arctic Conditions (POAC89), June 12-16, Luleå, Sweden.*
- Malmberg, S. (1983). "Om Fartygs Fastkilning I Is". MA thesis. Tekniska Högskolan, Maskiningenjörsavdelningen.
- Matusiak, J. (2010). *Laivan kulkuvastus*. Tech. rep. M-289. 4. korjattu painos. ISBN 978-952-60-3018-0.
- McGill, R., Remley, W., and Winther, K. (2013). *Alternative Fuels for Marine Applications*. Tech. rep. A Report from the IEA Advanced Motor Fuels Implementing Agreement.
- NASA (2015). *Globalwarming*. URL: <http://climate.nasa.gov/evidence/>.
- Northern Sea Route Information Office (2015). *NSR*. URL: <http://www.arctic-lio.com/NSR>.
- Omre, A. (2012). "An Economic Transport System of the Next Generation - Integrating the Northern And Southern Passages". MA thesis. Norwegian University of Science and Technology (NTNU).
- Otsuka, N., Izumiya, K., and Furuichi, M. (2013). "Study on Feasibility of the Northern Sea Route from Recent Voyages". In: *Proceedings, The 22nd International Conference on Port and Ocean Engineering Under Arctic Conditions, June 9-13, Espoo, Finland*.
- Riska, K. (2010a). *Design of Ice Breaking Ships*. Tech. rep. ILS Oy, Helsinki, Finland, University of Science, and Technology, Trondheim, Norway.
- Riska, K. (2010b). "Ship-Ice Interaction in Ship Design: Theory and Practice". In: *Encyclopedia of Life Support Systems (EOLSS), Paris, France*.
- Riska, K. (2014a). *Energy Efficiency of the Baltic Winter Navigation System*. Tech. rep. Winter Navigation Research Reports.
- Riska, K. (2014b). *The Influence of Ship Characteristics on Icebreaker Demand*. Tech. rep. Winter Navigation Research Reports.
- Riska, K., Wilhelmson, M., Englund, K., and Leiviskä, T. (1997). "Performance of Merchant Vessels in Ice in The Baltic". In: *Winter Navigation Research Board. Report No.52*.
- Sasaki, N., Laapio, J., Fagerström, B., Juurmaa, K., and Wilkamn, G. (2002). "Economical and environmental evaluation of double acting tanker". In: *Okhotsk Sea & Sea Ice*.
- Schartmüller, B. (2014). "A Simulation-Based Decision Support Tool for Arctic Transit Transport". MA thesis. Vienna University of Technology.

- Sillanpää, K. and Mäkiranta, J. (2014). "Internal Report R55-2a Definition of the 2025 and 2050 Ship Concepts: Arctic Cargo Vessel". In: *Joint Operation for Ultra Low Emission Shipping*.
- Statistics, N. I. of and Studies, E. (2015). *HFO Price*. URL: <http://www.insee.fr/en/bases-de-donnees/bsweb/serie.asp?idbank=001642883>.
- Stopford, M. (1997). *Maritime Economics*. 2nd. ISBN 0-415-15309-3 (hbk). Routledge.
- Strub-Klein, L. and Sudom, D. (2012). "A Comprehensive Analysis of the Morphology of First-Year Sea Ice Ridges". In: *Cold Regions Science and Technology*.
- Suez Canal Authority (2015). *SCR Toll*. URL: <http://www.suezcanal.gov.eg/calc.aspx#>.
- Sørstrand, S. S. (2012). "A Decision Support Model for Merchant Vessels Operating on the Arctic Sea". MA thesis. Norwegian University of Science and Technology (NTNU).
- Tan, X., Riska, K., and Moan, T. (2014). "Performance Simulation of a Dual-Direction Ship in Level Ice". In: *Journal of Ship Research*, Vol. 58, No. 3, pp. 1-14.
- Tõns, T., Erceg, S., Ehlers, S., and Leira, B. J. (2014). "Ice Condition Database for the Arctic Sea". In: *Proceedings of the ASME 2014 33rd International Conference on Ocean, Offshore and Arctic Engineering. OMAE 2014. June 8-13, San Francisco, California, USA*.
- United Nations Convention on the Law of the Sea (1982). *United Nations Convention on the Law of the Sea*. Article 234.
- U.S. National Ice Center (2015). *EGG code*. URL: http://www.natice.noaa.gov/products/egg_code.html.
- van Basshuysen, R. and Schäfer, F. (2004). *Internal Combustion Engine Handbook*. Sae International, Warrendale, Pa.
- Veitch, B., Kujala, P., Kosloff, P., and Leppäranta, M. (1991). *Field Measurements of the Thermodynamics of an Ice Ridge*. Tech. rep. Helsinki University of Technology. Laboratory of Naval Architecture and Marine Engineering. Report M-114.
- Veitch, B., Bose, N., Jordaan, I., Haddara, M., and Spencer, D (2003). "Chapter 40: Ice-Capable Ship". In: *Ship Design and Construction*. Ed. by T. Lamb.
- Verny, J. and Grigentin, C. (2009). "Container Shipping On the Northern Sea Route". In: *International Journal of Production Economics*. Elsevier.

- Vocke, M., Ranki, E., Uuskallio, A., Niini, M., and Wilkman, G. (2011). "Experience from Vessels Operating in Ice in the Double Acting Principle". In: *Arctic Technology Conference, OTC 900504, 7-9 February, Houston, Texas, USA*.
- von Bock und Polach, R. U. F., Ehlers, S., and Erikstad, S. O. (2014). "A Decision-based Design Approach for Ship Operating in Open Water and Ice". In: *Journal of Ship Production and Design, Vol. 30, No. 3, August 2014, pp. 1-11*.
- Way, B., Khan, F., and Veitch, B. (2015). "The Northern Sea Route vs. The Suez Canal Route - An Economic Analysis Incorporating Probabilistic Simulation Optimization of Vessel Speed". In: *Proceedings of the ASME 2015 34th International Conference on Ocean, Offshore and Arctic Engineering, OMAE2015, May 31 - June 5, 2015, St. John's, Newfoundland, Canada*.
- Weeks, W. F. (2010). *On Sea Ice*. University of Alaska Press.
- Wärtsilä (2015). *Wärtsilä Solutions For Marine And Oil & Gas Markets*. Wärtsilä.

Appendix A

Ice data

Ice data (Arpiainen and Kiili 2006)

Bering Strait					
		Ice thickness [m]	Concentration [%]	Mean ridge thickness [m]	Ridges/km
Jan	average	0.3	98	3	3
	severe	0.9	98	4	4
Feb	average	0.4	98	4	3
	severe	1	98	6	4
Mar	average	0.5	98	4	3
	severe	1.1	98	6	4
Apr	average	0.6	98	4.5	3
	severe	1.2	98	6	4
May	average	0.6	98	4.5	3
	severe	1.2	98	6	4
Jun	average	0.5	95	4.5	3
	severe	1.1	98	6	4
Jul	average	0	0	0	0
	severe	0.8	90	6	4
Aug	average	0	0	0	0
	severe	0.3	60	6	4
Sep	average	0	0	0	0
	severe	0	0	0	0
Oct	average	0	0	0	0
	severe	0	0	0	0
Nov	average	0	0	0	0
	severe	0.4	95	3	4
Dec	average	0.2	85	2	3
	severe	0.8	98	3	4

Chukchi

		Ice thickness [m]	Concentration [%]	Mean ridge thickness [m]	Ridges/km
Jan	average	1.1	98	5	5
	severe	1.7	98	7	7
Feb	average	1.4	98	6	5
	severe	1.8	98	10	7
Mar	average	1.6	98	9	5
	severe	1.9	98	10	7
Apr	average	1.8	98	9	5
	severe	2	98	10	7
May	average	1.8	98	9	5
	severe	2	98	10	7
Jun	average	1.7	95	9	5
	severe	1.9	98	10	7
Jul	average	0.5	30	9	5
	severe	1.2	90	10	7
Aug	average	0	0	0	0
	severe	0.8	80	10	7
Sep	average	0	0	0	0
	severe	0.4	50	10	7
Oct	average	0	0	0	0
	severe	0.9	80	6	7
Nov	average	0.3	85	4	5
	severe	1.3	95	6	7
Dec	average	0.8	85	4	5
	severe	1.6	98	6	7

East Siberia

		Ice thickness [m]	Concentration [%]	Mean ridge thickness [m]	Ridges/km
Jan	average	1.5	98	6	4
	severe	2	98	7	6
Feb	average	1.8	98	8	4
	severe	2.3	98	8	6
Mar	average	2.0	98	9	4
	severe	2.4	98	9	6
Apr	average	2.2	98	9.9	4
	severe	2.6	98	10	6
May	average	2.2	98	9.9	4
	severe	2.6	98	10	6
Jun	average	2.1	95	9.9	4
	severe	2.5	98	10	6
Jul	average	1.1	80	9.9	4
	severe	1.7	90	10	6
Aug	average	1	30	9.9	4
	severe	1.2	80	10	6
Sep	average	0	0	0	0
	severe	0.9	50	10	6
Oct	average	0	0	0	0
	severe	1.1	80	6	6
Nov	average	0.4	85	5	4
	severe	1.4	95	6	6
Dec	average	0.9	90	5	4
	severe	1.7	98	6	6

Laptev

		Ice thickness [m]	Concentration [%]	Mean ridge thickness [m]	Ridges/km
Jan	average	0.6	98	5.5	3
	severe	1.6	98	6	5
Feb	average	0.8	98	7	3
	severe	1.8	98	7	5
Mar	average	1	98	7	3
	severe	2	98	8	5
Apr	average	1.3	98	7.7	3
	severe	2.1	98	8.5	5
May	average	1.3	98	7.7	3
	severe	1.8	98	8.5	5
Jun	average	1.2	95	7.7	3
	severe	1.7	98	8.5	5
Jul	average	0.7	70	7.7	3
	severe	1.3	90	8.5	5
Aug	average	0.5	30	7.7	3
	severe	0.8	80	8.5	5
Sep	average	0	0	0	0
	severe	0.6	50	8.5	5
Oct	average	0	0	0	0
	severe	1	80	5	5
Nov	average	0.5	85	5	3
	severe	1.4	95	5	5
Dec	average	1	90	5	3
	severe	1.5	98	5	5

Kara East

		Ice thickness [m]	Concentration [%]	Mean ridge thickness [m]	Ridges/km
Jan	average	1	98	6	5
	severe	1.8	98	7	7
Feb	average	1.2	98	8	5
	severe	2	98	8	7
Mar	average	1.4	98	10	5
	severe	2.1	98	9	7
Apr	average	1.4	98	10	5
	severe	2.2	98	10	7
May	average	1.4	98	10	4
	severe	2.2	98	10	7
Jun	average	1.3	95	10	5
	severe	2.1	98	10	7
Jul	average	0.8	40	10	5
	severe	1.5	90	10	7
Aug	average	0	0	0	0
	severe	1.1	80	10	7
Sep	average	0	0	0	0
	severe	0.6	50	10	7
Oct	average	0	0	0	0
	severe	0.9	80	7	7
Nov	average	0.3	85	5	5
	severe	1.3	95	7	7
Dec	average	0.7	85	5	5
	severe	1.6	98	7	7

Kara Centre

		Ice thickness [m]	Concentration [%]	Mean ridge thickness [m]	Ridges/km
Jan	average	0.9	98	4	2
	severe	1.5	98	6	3
Feb	average	1.2	98	5	2
	severe	1.6	98	8.8	3
Mar	average	1.3	98	5	2
	severe	1.7	98	8.5	3
Apr	average	1.3	98	5.6	2
	severe	1.8	98	8.5	3
May	average	1.3	98	5.6	2
	severe	1.8	98	8.5	3
Jun	average	1.2	95	5.6	2
	severe	1.7	98	8.5	3
Jul	average	0.7	40	5.6	2
	severe	1.2	90	8.5	3
Aug	average	0	0	0	0
	severe	0.8	75	8.5	3
Sep	average	0	0	0	0
	severe	0.5	40	8.5	3
Oct	average	0	0	0	0
	severe	0.8	80	5	3
Nov	average	0.2	85	3	2
	severe	1.2	95	5	3
Dec	average	0.6	85	3	2
	severe	1.4	98	5	3

Kara West

		Ice thickness [m]	Concentration [%]	Mean ridge thickness [m]	Ridges/km
Jan	average	0.6	98	4	2
	severe	1.3	98	5	3
Feb	average	0.8	98	5	2
	severe	1.4	98	8	3
Mar	average	1	98	5	2
	severe	1.5	98	8	3
Apr	average	1	98	5.6	2
	severe	1.5	98	8	3
May	average	1	98	5.6	2
	severe	1.5	98	8	3
Jun	average	0.9	95	5.6	2
	severe	1.4	98	8	3
Jul	average	0.7	20	5.6	2
	severe	0.8	90	8	3
Aug	average	0	0	0	0
	severe	0.6	65	8	3
Sep	average	0	0	0	0
	severe	0.1	40	8	3
Oct	average	0	0	0	0
	severe	0.3	80	3	3
Nov	average	0.1	85	3	2
	severe	1	95	3	3
Dec	average	0.4	85	3	2
	severe	1.2	98	3	3

Kara Gate

		Ice thickness [m]	Concentration [%]	Mean ridge thickness [m]	Ridges/km
Jan	average	0.5	98	4	6
	severe	1.1	98	6	7
Feb	average	0.6	98	6	6
	severe	1.2	98	10	7
Mar	average	0.7	98	6	6
	severe	1.3	98	10	7
Apr	average	0.7	98	6.7	6
	severe	1.3	98	10	7
May	average	0.7	98	6.7	6
	severe	1.3	98	10	7
Jun	average	0.6	95	6.7	6
	severe	1.2	98	10	7
Jul	average	0.4	30	6.7	6
	severe	0.8	90	10	7
Aug	average	0	0	0	0
	severe	0.6	60	10	7
Sep	average	0	0	0	0
	severe	0.3	40	10	7
Oct	average	0	0	0	0
	severe	0.2	80	4	7
Nov	average	0	0	0	0
	severe	0.5	95	4	7
Dec	average	0.3	85	4	6
	severe	1	98	4	7

Pechora

		Ice thickness [m]	Concentration [%]	Mean ridge thickness [m]	Ridges/km
Jan	average	0.4	98	3	2
	severe	0.5	98	4	3
Feb	average	0.5	98	4	2
	severe	0.6	98	6	3
Mar	average	0.6	98	4	2
	severe	0.7	98	6	3
Apr	average	0.6	98	4.5	2
	severe	0.7	98	6	3
May	average	0.7	98	4.5	2
	severe	0.7	98	6	3
Jun	average	0.6	95	4.5	2
	severe	0.6	98	6	3
Jul	average	0	0	0	0
	severe	0.4	90	6	3
Aug	average	0	0	0	0
	severe	0	0	0	0
Sep	average	0	0	0	0
	severe	0	0	0	0
Oct	average	0	0	0	0
	severe	0	0	0	0
Nov	average	0	0	0	0
	severe	0.2	95	3	3
Dec	average	0.3	85	3	2
	severe	0.4	98	3	3